Compositional characteristics and spatial distribution of enriched Icelandic mantle components

David W. Peate [1], Kresten Breddam [2], Joel A. Baker [3],

Mark D. Kurz [4], Abigail K. Barker [5], Tore Prestvik [6],

Nathalie Grassineau [7] & Anna Cecilie Skovgaard [8].

1 Department of Geoscience, 121 Trowbridge Hall, University of Iowa, Iowa City, IA 52242, USA.

2 Statens Institut for Strålehygiejne, Knapholm 7, 2730 Herlev, DENMARK.

3 School of Geography, Environment and Earth Sciences, Victoria University of Wellington, P.O. Box 600, Wellington, NEW ZEALAND.

4 Marine Chemistry & Geochemistry Department, Woods Hole Oceanographic Institution, Woods Hole, MA 02543, USA.

5 Department of Earth Sciences, Uppsala University, Villavägen 16, SE 752 36, Uppsala, SWEDEN.

6 Institute for Geology and Mineral Resources Engineering, Norwegian University of Science and Technology, N-7491 Trondheim, NORWAY.

7 Department of Geology, Royal Holloway University of London, Egham, Surrey TW20 0EX, UK.

8 Danish Environmental Protection Agency, 1401 Copenhagen, DENMARK.

* corresponding author: David W. Peate e-mail: david-peate@uiowa.edu

tel.: (319) 335 0567 fax: (319) 335 1821

revised version for ***Journal of Petrology*** *(March 2010)*

word counts:	*abstract:*	*395*	
	main text:	*10635*	
	references:	*3315*	*(120 references)*
	figure & table captions:	*1152*	*(9 figures, 6 tables)*

ABSTRACT

We present compositional data on a suite of 18 primitive neovolcanic alkali basalts from three flank zone regions in Iceland (Vestmannaeyjar in the south, Snæfell in the east, and Snæfellsnes in the west) that are peripheral to the main rift zones that are dominated by tholeiitic basalts. This study integrates He isotope data with radiogenic isotope data (Sr-Nd-Pb-Hf), stable isotope data ($\delta^{18}O$), and trace element data to characterise the compositional features of the trace-element-enriched components of the Icelandic mantle. We also present high-precision Pb isotope data on an additional 57 lava samples from the flank zones (including Öræfajökull in the south-east) and the Northern and Eastern rift zones. Most Icelandic lavas have negative $\Delta^{207}Pb$ (–4 to –1), with higher values (–1 to +4) found only in samples from Öræfajökull, Snæfell, and parts of the Reykjanes Peninsula. At Snæfell, this EM1-type component is characterised by a low $\delta^{18}O_{olivine}$ signature (+4.1‰ to +4.6‰), moderate $^{206}Pb/^{204}Pb$ values (18.4-18.6) and MORB-like $^{3}He/^{4}He$ (6.9-7.5 R/R_A). Samples from Vestmannaeyjar and Snæfellsnes have mantle-like $\delta^{18}O_{olivine}$ (+4.9‰ to +5.0‰), and radiogenic $^{206}Pb/^{204}Pb$ values (18.9-19.3) that fall on the NHRL for $^{208}Pb/^{204}Pb$ ($\Delta^{208}Pb$ –5 to +5). Compared to the Vestmannaeyjar lavas, Snæfellsnes lavas have higher La/Yb_N (5-11 vs. 3-5), lower ε_{Nd} (5.5-6.5 vs. 6.8-7.6) and lower $^{3}He/^{4}He$ (6.3-8.6 R/R_A vs. 11.4-13.5 R/R_A). Therefore, the most trace element enriched components in the Icelandic mantle are not the carriers of the high $^{3}He/^{4}He$ values (> 15 R/R_A) found in some lavas on Iceland and the adjacent ridges, and instead are consistent with degassed, recycled components. Even after excluding the EM1-type high $\Delta^{207}Pb$ samples, high-precision Pb isotope data produce a kinked array on an $^{206}Pb/^{204}Pb$ vs. $^{208}Pb/^{204}Pb$ plot, which is not consistent with simple binary mixing between two end-members. This requires significant lateral heterogeneity within the Icelandic mantle and the presence of more than just two compositionally-distinct local mixing end-member components. Samples from each of the main axial rift zones define different trends. Despite the tectonic continuity between the Northern Volcanic Zone and the Eastern Volcanic Zone, lavas from these two rift zones define separate sub-parallel linear arrays. Lavas from the adjacent Western Volcanic Zone and the Eastern Volcanic Zone define oblique linear arrays that converge on a common local end-member that is not involved in the magmatism of the Northern Volcanic Zone. Therefore, there is a distinct NE-SW compositional heterogeneity within the Icelandic mantle.

key words: *Iceland, He isotopes, Pb isotopes, O isotopes, flank zone lavas, rift zone lavas.*

1. INTRODUCTION

The petrological diversity of recent Icelandic mafic lavas is linked to the dynamic local tectonic environment (e.g. *Jakobsson, 1972*). Post-glacial magmatism (younger than ~13,000 years) is largely confined to a series of well-defined neovolcanic zones (Fig. 1). The Northern Volcanic Zone (NVZ) and Western Volcanic Zone (WVZ), which represent the onshore continuation of the offshore Kolbeinsey Ridge and Reykjanes Ridge respectively, are dominated by tholeiitic basalts together with rare picrites. In contrast, the southward-propagating Eastern Volcanic Zone (EVZ), particularly the offshore islands of Vestmannaeyjar, and the other flank zones or off-axis zones to the east (Snæfell-Öræfajökull) and west (Snæfellsnes) are dominated by transitional to alkali basalts.

A compilation of rare earth element data from various sources (Fig. 2a) illustrates the compositional contrasts between the lavas of the axial rift zones and those of the flank zones. In general, the flank zone lavas have higher La/Yb and Dy/Yb than the axial rift zone lavas, indicating that they were generated by smaller degrees of melting at greater average depths (e.g. *Kokfelt et al., 2006*). These data are consistent with the thicker lithospheric lid beneath the flank zones that limits the extent of decompression melting relative to the axial rift zones. However, these trace element variations are also correlated with radiogenic isotope compositions (e.g. Nb/Zr vs. $^{143}Nd/^{144}Nd$: Fig. 2b) which requires a role for mantle heterogeneity. One model to explain the compositional variations of Icelandic lavas involves variable degrees of melting of a heterogeneous mantle composed of lower solidus, enriched veins or 'blobs' set in a more refractory, depleted matrix (e.g. *Chauvel & Hémond, 2000; Fitton et al., 2003; Stracke et al., 2003; Kokfelt et al., 2006*). Small degrees of melting beneath the flank zones will preferentially sample the more fusible enriched veins, while larger degrees of melting beneath the axial rift zones allow a greater contribution from the more depleted matrix.

However, lead isotope data indicate that the Icelandic mantle is heterogeneous on a more complex scale than this simple two-component mixture (e.g. Fig. 2c), with more than just one ‘depleted’ and one ‘enriched’ component recognised (e.g. *Hanan & Schilling, 1997; Thirlwall et al., 2004*). High precision Pb isotope data (*Thirlwall et al., 2004; Baker et al., 2004; Kitagawa et al., 2008; Peate et al., 2009*) allow local mantle end-member components to be resolved within individual volcanic systems. The compositional features and spatial relationships of these components can provide information about the origin, distribution and length scales of

heterogeneities within the mantle.

A long recognised feature of Iceland is the high $^3He/^4He$ values of the lavas compared with the surrounding ridges (e.g. *Condomines et al., 1983; Kurz et al., 1985; Schilling et al., 1999; Hilton et al., 2000*), with the highest values ($^3He/^4He$ of 38-43 R/R_A) found in the ~15 Ma lavas of NW Iceland (*Hilton et al., 1999; Breddam & Kurz, 2001*). Most workers have attributed this high $^3He/^4He$ signature to a 'plume component' bringing undegassed primordial material from the deep mantle, especially as it is also associated with solar Ne isotope ratios (e.g. *Dixon et al., 2000; Moreira et al., 2001*). However, the compositional diversity of components present in the Icelandic mantle, as recognised from the high precision Pb isotope data, means that it is difficult to identify a single deep mantle 'plume component' at Iceland. An important question, therefore, is whether the high $^3He/^4He$ signature is specifically associated with any of the incompatible trace element enriched components. Several recent studies of Icelandic magmatism and the earlier magmatism of the North Atlantic Igneous Province have in fact linked elevated $^3He/^4He$ values with more incompatible trace element depleted compositions (*Stuart et al., 2003; Ellam & Stuart, 2004; Macpherson et al., 2005*).

In order to address these issues, we present new He isotope data and high precision Pb isotope data, together with accompanying major and trace element data and Sr-Nd-Hf-O isotope data, for primitive (MgO-rich) incompatible trace element enriched basalts from the flank zones in Iceland. We also provide high precision Pb isotope data on other post-glacial samples from throughout Iceland to place the Pb isotope composition of the flank zone samples into a more regional Icelandic context and as a means to establish a better picture of lateral compositional heterogeneity in the mantle beneath Iceland. In particular, we highlight differences in Pb isotope composition of the mantle feeding the three main neovolcanic rift zones (WVZ, NVZ & EVZ).

2. ICELANDIC FLANK ZONES AND SAMPLE DETAILS

The flank zones have several features in common. They show poorly developed extensional tectonics, and the volcanic products lie unconformably on older tholeiitic lava successions (up to 10 Ma). The flank zone eruptions show evidence of magmatic evolution at mid-crustal levels (13-30 km) as indicated by lava compositions (*Furman et al., 1991; Hards et al., 2000*), seismic data (*Gebrande et al., 1980*), and the lack of associated high-T hydrothermal activity. However, the tectonic settings of the individual zones differ (Fig. 1): Vestmannaeyjar are located on the propagating rift of the Eastern Volcanic Zone; Snæfell and Öræfajökull may represent sites of

incipient rifting above the fringe of the plume; and Snæfellsnes is situated in an old leaky transform (*Oskarsson et al., 1982; Hards et al., 2000; Mattsson & Oskarsson, 2005*).

We present comprehensive elemental and isotopic data on 18 samples from these three flank zones. In the absence of gas-rich sub-glacial glass samples, olivine-rich lavas were targeted, as He isotopic ratios can be measured on gas liberated from inclusions in olivine crystals. In order to avoid or limit *in-situ* cosmogenic ^{3}He production, samples were collected within quarries, road cuts, fresh rock falls, or lava tunnels where possible. The primitive compositions (MgO 7.9-15.3 wt%) of the samples also serves to minimize potential crustal contamination problems frequently observed in more fractionated Icelandic lavas (e.g. *Condomines et al., 1983; Bindeman et al., 2008*). Additional samples from the Northern Volcanic Zone and the Eastern Volcanic Zone (from *Kurz et al., 1985; Breddam et al., 2000; Skovgaard et al., 2001)* were analysed for high-precision Pb isotopes. These Pb isotope data complement high-precision double-spike analyses from *Thirlwall et al. (2004)*, *Baker et al. (2004, 2005)* and *Peate et al. (2009)* to provide a more comprehensive sample coverage of the neovolcanic zones of Iceland.

The Vestmannaeyjar flank zone (including Katla and Eyjafjöll), part of the Eastern Volcanic Zone, comprises several active volcanic systems that become increasingly alkaline southwards, with the offshore Vestmannaeyjar as the most alkaline end-member (*Jakobsson, 1972*). On the Vestmannaeyjar, only Heimaey was sampled for this study. Fresh rock falls were abundant on Heimaey due to the South Iceland magnitude 6.6 earthquake in 2000. An ankaramite lava flow from an old quarry at Hvammsmuli, Eyjafjöll (*Steinthorsson, 1964*) on the mainland 20 km NE of Heimaey is discussed together with the Heimaey samples. Within the Snæfellsnes flank zone, lavas become increasingly alkaline from east to west, with Snæfellsjökull as the most alkaline end-member (*Steinthorsson et al., 1985*), and there are also systematic east-west changes in Sr isotopic ratios that suggest a gradational change in mantle source composition (*Sigmarsson et al., 1992*). Representative mafic samples were collected along the length of the Snæfellsnes Peninsula.

Of the two main centres within the Snæfell-Öræfajökull flank zone, high MgO basalts were only found at Snæfell. Snæfell is a bimodal central volcanic complex (~0.3 Ma: *Guillou et al., 2010*), and mildly alkaline olivine-rich basalts were erupted along a poorly developed fissure swarm (*Hards et al., 1995; 2000*). Suitable localities were rare at Snæfell, due to the heavily ice-eroded faces, and sampling rarely took place more than 0.5 metres below the surface. The

Öræfajökull central volcano is dominated by evolved lavas (MgO < 6 wt%), unsuitable for He isotope study, but because of their anomalous Sr-Pb isotope compositions (*Prestvik et al., 2001*), we re-analysed these samples for high precision Pb isotope compositions.

3. ANALYTICAL METHODS

A total of 18 flank-zone samples were crushed in a tungsten carbide jaw crusher, and then powdered in an agate mill. Major elements were analysed by X-ray-fluorescence on fused glass discs using a Phillips PW1606 spectrometer at the Geological Survey of Denmark and Greenland, except Na_2O (atomic absorption spectroscopy) and FeO (wet titration) (see *Kystol & Larsen, 1999*, for full details of methodologies and analytical precision). Trace elements were analysed by inductively-coupled plasma mass spectrometry, using a Thermo X-series II instrument at the University of Iowa. 0.1g of rock powder was digested with HF-HNO_3, and run in 2% HNO_3 at a dilution factor of 5000, after spiking with internal standards (Be, Rh, In, Re, Bi). Data reduction included corrections for machine drift, reagent blanks, oxide interferences and isotopic overlaps. The data were calibrated with four rock standard reference materials (BHVO-1, BCR-2, AGV-2, BIR-1), using the preferred values from the GeoReM database (http://georem.mpch-mainz.gwdg.de/). Precision and accuracy can be assessed from replicate analyses of standard reference materials analysed as unknown samples. Results for BRP-1 and JA-1 are provided in Table 1. The accuracy relative to the GeoReM preferred values is <5% for all elements except Cr, Ni, Th, Ta, Nb. The precision (2 r.s.d.) of replicate analyses is <3% for all elements except Rb, Y, La, Ga (<5%) and Sc, Cr, Cs, Th, U (<12%).

Helium isotope analyses were carried out on olivine separates at Woods Hole Oceanographic Institution. Helium in olivine resides primarily within inclusions and can be extracted simply by crushing. The advantage of the crushing method over the step heating method is that only the inherited magmatic He contained in inclusions is released by the crushing method, in contrast to step heating measurements where both radiogenic ^{4}He (produced by U and Th decay) and cosmogenic ^{3}He can be released from the crystal matrix (e.g. *Kurz, 1986*). Fresh olivine phenocrysts were hand-picked to exclude crystals with altered surfaces or secondary mineral coatings. Large crystals (~2-3 mm) were picked where possible in order to favor high gas concentrations. After ultrasonic cleaning (10 min.) in acetone and air drying, 250-300 mg phenocrysts were placed in stainless steel crushers designed for *in vacuo* crushing and connected to the mass spectrometer. Complete analytical details can be found in *Kurz & Geist (1999)*.

Sr-Nd-Hf-Pb isotope analyses were performed on a VG Axiom MC-ICP-MS at the Danish Lithosphere Centre. Hand-picked 0.5-1.0 mm rock chips were used for Sr-Nd-Pb isotope analyses to avoid potential contamination problems from crushing procedures. The chips were leached in hot 6M HCl for 1-2 hours and rinsed thoroughly in MQ H_2O. This procedure was repeated several times until there was no visible coloration of the HCl. The chips were digested using HF, HNO_3 and HCl. A ^{207}Pb-^{204}Pb double spike was used to correct Pb isotope ratios for mass bias (details in *Baker et al., 2004*). The external reproducibility of Pb isotope ratios for NIST SRM981 was < ± 200 ppm, and replicate analyses of samples had similar reproducibility. Sr was separated using cation exchange followed by a Rb and HREE clean-up procedure using Eichrom Sr-spec resin. An on-peak zero measurement method was used to correct for the ^{86}Kr interference on ^{86}Sr, and $^{87}Sr/^{86}Sr$ data were corrected for instrumental mass fractionation using $^{86}Sr/^{88}Sr = 0.1194$ (details in *Waight et al., 2002*). External reproducibility of $^{87}Sr/^{86}Sr$ for NIST SRM987 was better than ± 0.000025 (2 s.d.), and data are presented relative to a value of 0.71025 for this standard. Nd isotopes were analysed on the REE column cuts (unseparated Sm-Nd fractions) from the Sr cation ion-exchange columns after a Ba clean-up, following the general methodology of *Luais et al. (1997)*. Nd isotope ratios were corrected for instrumental mass fractionation using $^{146}Nd/^{145}Nd = 2.071943$, as both masses are free of Sm isobaric interferences. Nd isotopes are reported relative to an Ames Nd metal standard $^{143}Nd/^{144}Nd = 0.51213$, equivalent to 0.51186 for La Jolla. External reproducibility for $^{143}Nd/^{144}Nd$ was better than ± 0.000010 (2 s.d.). Procedural blanks for Nd were 20 to 33 pg. Hf isotopes were analysed using the method described in *Ulfbeck et al. (2003)*. Hand picked rocks chips (< 0.5 mm) were weighed into pre-ignited graphite crucibles with lithium metaborate flux, and fused for 5 to 10 minutes at 1100 ºC. The melt was completely dissolved in 2M HCl, and then processed through cation exchange columns and TEVA-spec columns to isolate a Hf fraction. Hf isotopes are reported to an internal Hf standard of $^{176}Hf/^{177}Hf = 0.28189$, equivalent to JMC 475 = 0.282160. Total Hf procedural blanks were 42 to 166 pg.

Oxygen isotope data were obtained at Royal Holloway University of London using a LaserPrep system on line to a VG Optima dual inlet mass spectrometer (*Mattey & Macpherson, 1993; Thirlwall et al., 2006*). Pure mineral separates (1.7 mg) were combusted via a Synrad CO_2 laser in the presence of excess BF_5. Oxygen yields for olivine were 90-97% and for clinopyroxene and plagioclase were 95-98%. The San Carlos Olivine II standard gave $\delta^{18}O$ of

5.24 ± 0.09 ‰ (n=11), and the GMG II standard gave $\delta^{18}O$ of 5.72 ± 0.03 ‰ (n=5), which are calibrated against the NBS-30 biotite at +5.1‰. The overall precision on standards and sample replicates is better than ±0.1‰. All $\delta^{18}O$ values are reported relative to V-SMOW.

4. RESULTS

4.1 Major and trace elements

The flank zone samples are all slightly vesicular basalts with phenocrysts of olivine ± plagioclase, and ± clinopyroxene, embedded in a fine to medium grained groundmass of olivine, plagioclase, clinopyroxene and oxides. The sample from Hvammsmuli is a highly porphyritic ankaramite lava, with ~20% phenocrysts of olivine and clinopyroxene, both typically 1-4 mm in size (see Steinthórsson, 1964).

Major and trace element data are presented in Table 2. The samples are among the most primitive (MgO: 7.9-15.3 wt %) transitional to alkali basalts found in Iceland (*Furman et al., 1991; Hémond et al., 1993; Hards et al., 1995, 2000; Mattsson & Oskarson, 2005*). Relative to primitive Icelandic olivine tholeiites of comparable MgO content, these lavas have similar abundances of Ni (110-420 ppm) Cr (340-1000 ppm), Al_2O_3 (12.2-15.5 wt%) and FeO (9.6-12.2 wt %), lower SiO_2 (45.8-48.1 wt %) and CaO (10.5-11.8 wt %) and higher TiO_2 (1.6-3.3 wt %), Na_2O (1.8-2.8 wt %), K_2O (0.3-0.9 wt %) and P_2O_5 (0.2-0.5 wt %). The samples have higher Na_2O+K_2O than the tholeiites but plot on or below the alkaline-subalkaline division line on a total alkalis-silica classification diagram (Fig. 3a), demonstrating their subalkaline nature. However, following the established practice we denote these incompatible trace element rich Icelandic lavas as 'alkali basalts'.

The alkali basalts have higher incompatible trace element abundances (~2-50x) than typical ol-tholeiites from the rift zones, but with similar geochemical features such as positive Nb, Ta anomalies and negative Cs, K, Pb and P anomalies on a primitive-mantle-normalised diagram (Fig. 3b). One notable difference is the lack of positive Sr anomalies in the alkali basalts, which contrasts with most tholeiites in Iceland (e.g. *Hémond et al., 1993; Breddam, 2002*). At similar MgO contents (~11 wt%) Snæfell and Snæfellsnes have 2-4 times higher contents of the most incompatible trace elements relative to Vestmannaeyjar (Fig. 3b). In detail, there are differences in incompatible element ratios between our samples from the three flank zones (Fig. 2a). Lavas from Heimaey have the lowest La/Yb_N (~3), with Dy/Yb_N ~1.4. The Hvammsmuli sample has

higher La/Yb_N (~5) and Dy/Yb_N ~1.7, similar to published values from the nearby volcanic centres at Eldja and Hekla (*Kokfelt et al., 2006*). The Snæfellsnes samples show a wide range in La/Yb_N (~5-11), at similar Dy/Yb_N (~1.3-1.5) to Heimaey. Snæfell lavas have similar La/Yb_N (~6-8) to some of the Snæfellsnes samples, but with higher Dy/Yb_N (~1.6) and also higher La/Nb and Th/Nb and lower Nb/U. Published analyses of mafic samples (5-6 wt% MgO) from Öræfajökull (*Prestvik et al., 2001*) show similar Dy/Yb_N to Snæfell lavas, but with lower La/Yb_N (~3-6).

4.2 High precision Pb isotope data

The double-spike Pb isotope data are presented in Table 3, and these data are plotted in Fig. 4 together with double-spike data from *Thirlwall et al. (2004)*, *Baker et al. (2004, 2005)* and *Peate et al. (2009).* The observed range in $^{206}Pb/^{204}Pb$ for all Icelandic lavas (17.92 to 19.30) is similar to that seen in previously published Pb isotope data, but with significantly reduced variation in $^{207}Pb/^{204}Pb$ and $^{208}Pb/^{204}Pb$ for a given $^{206}Pb/^{204}Pb$ value as a result of the better control on instrumental mass fractionation given by the double-spike method over conventional TIMS analyses. For the flank zone lavas, samples from the Snæfell-Öræfajökull flank zone have intermediate $^{206}Pb/^{204}Pb$ compositions (18.43 to 18.66), compared to the radiogenic values found in the Snæfellsnes flank zone lavas and Heimaey-Hvammsmuli lavas (18.82 to 19.24).

Most Icelandic lavas plot on a tight linear array below the NHRL (Northern Hemisphere Reference Line: *Hart, 1984*) on a $^{207}Pb/^{204}Pb$ vs. $^{206}Pb/^{204}Pb$ diagram (Fig. 4a), and over 85% of the analyses have negative $\Delta^{207}Pb$ (where $\Delta^{207}Pb$ is the vertical deviation of a sample from the NHRL x 100: *Hart, 1984*). Anomalous positive $\Delta^{207}Pb$ (and $\Delta^{208}Pb$) values of lavas from Öræfajökull have been documented by conventional TIMS analyses (*Prestvik et al., 2001*), and these features are confirmed by the new high-precision double-spike data on the same samples (Fig. 4b: $\Delta^{207}Pb$ 1.8 to 4.0). Lavas from Snæfell also have resolvably higher $\Delta^{207}Pb$ values (–0.7 to 1.1) than any other Icelandic lavas except those from Öræfajökull and parts of the Reykjanes Peninsula (*Thirlwall et al., 2004; Peate et al., 2009*). Most samples from the Eastern Volcanic Zone (including Heimaey and Hvammsmuli) and from the Snæfellsnes flank zone plot along the NHRL from $^{206}Pb/^{204}Pb$ of 18.8 to 19.2 on a $^{208}Pb/^{204}Pb$ vs. $^{206}Pb/^{204}Pb$ diagram (Fig. 4c), with $\Delta^{208}Pb$ values of –8 to +7 (Fig. 4d). The Northern Volcanic Zone lavas have $^{206}Pb/^{204}Pb$ compositions from 17.92 to 18.51 and form an array sub-parallel to the NHRL but displaced to higher $^{208}Pb/^{204}Pb$ ($\Delta^{208}Pb$ of 19 to 31). Lavas from Snæfell and Öræfajökull form trends oblique

to the NHRL, with higher Δ^{208}Pb at lower ^{206}Pb/^{204}Pb, but the Öræfajökull trend is displaced to higher ^{208}Pb/^{204}Pb (Δ^{208}Pb of 34 to 52) compared to Snæfell (Δ^{208}Pb of 18 to 32).

4.3 Helium isotope data

Helium concentrations in the olivines vary significantly (0.1–16.3 x 10^{-9} cm^3 STP/g: Table 4) and overlap with the range found in other studies of Icelandic olivines (see dotted field on Fig. 5a). These values are about an order of magnitude lower than in Icelandic subglacial glasses (e.g. *Kurz et al., 1985; Breddam et al., 2000*). Olivine samples from each alkaline centre show almost identical ^{3}He/^{4}He over a wide range of He contents, suggesting that radiogenic ingrowth, atmospheric contamination or *in situ* ^{3}He production are all insignificant (Fig. 5a). Helium isotopic ratios in alkali basalts have previously been reported on only one sample from Snæfellsnes (ol 7.5 R/R_A; cpx 6.9 R/R_A), two samples from Öræfajökull (ol 7.7-8.0 R/R_A), one sample from Snæfell (ol 7.1 R/R_A) and four samples from Vestmannaeyjar (ol 11.0-15.1 R/R_A) (*Kurz et al., 1985; Poreda et al., 1986; Sigmarsson et al., 1992; Debaille et al., 2009*). The new data confirm that the alkaline lavas from the Vestmannaeyjar flank zone have elevated He isotopic ratios relative to the nominal MORB range (7–9 R/R_A: *Graham, 2002*). The ^{3}He/^{4}He in the samples from Heimaey varies between 13.1 and 14.5 R/R_A, in good agreement with earlier results, and a value of 17.1 R/R_A was obtained for Hvammsmuli (Eyjafjöll) close to the range previously found at Eyjafjöll and Katla (16.8-19.4 R/R_A: *Wiese, 1992; Debaille et al., 2009*). In contrast, the ^{3}He/^{4}He ratios observed at Snæfell (6.9-7.5 R/R_A) and Snæfellsnes (6.3-8.6 R/R_A) are within the MORB range, but below the nominal MORB value. These results are consistent with the measured helium isotope compositions of hydrothermal fluids in the three flank zone regions (Snæfellsnes & Snæfell, < 10 R/R_A; Vestmannaeyjar, 10-18 R/R_A: *Hilton et al., 1990*), indicating that mantle-derived helium is being supplied to these hydrothermal systems. Similar MORB-like He isotope compositions have also been measured in incompatible trace element enriched basalts at the southern end of the Northern Volcanic Zone in central Iceland (*Macpherson et al., 2005*).

4.4 Sr-Nd-Hf isotope data

The Sr and Nd isotope data are presented in Table 4, and the Hf isotope data are presented in Table 5. In terms of Nd and Hf isotope compositions, the flank zone lavas plot at the unradiogenic end of the data array shown by Icelandic rift zone lavas (Fig. 6b), but each area has a distinct composition. Samples from Snæfellsnes, Snæfell and Öræfajökull plot above the

mantle array, similar to the rift zone lavas (*Stracke et al., 2003; Blichert-Toft et al., 2005; Table 5)*. Öræfajökull samples have lower εNd and εHf (6.0-6.4 and 11.5-12.0) than Snæfell samples (6.5-7.0 and 13.5-13.9), and overlap the compositions of Snæfellsnes samples (5.6-6.5 and 12.0-12.8). Samples from Heimaey and Hvammsmuli plot on or below the mantle array, with εNd of 6.8-7.6 and εHf of 11.4-13.5. Snæfell samples have higher $^{87}Sr/^{86}Sr$ (0.70347-0.70360) and εNd compared to Snæfellsnes samples (0.70336-0.70350), while samples from Heimaey have the lowest $^{87}Sr/^{86}Sr$ (0.70314-0.70320). These Sr-Nd isotope data are consistent with other published analyses from these areas (e.g. *Furman et al., 1991, 1995; Sigmarsson et al., 1992; Hémond et al., 1993; Hards et al., 1995, 2000; Kokfelt et al., 2006;* and references therein), except for Snæfell for which our $^{87}Sr/^{86}Sr$ values are ~0.0002 higher than those determined by *Hards et al. (1995, 2000)*.

4.5 Oxygen isotope data

Multiple mineral phases (olivine, clinopyroxene, plagioclase) were analysed for $\delta^{18}O$ where possible (see Table 4). Two samples from Snæfell gave $\Delta^{18}O_{plag-ol}$ values of +0.66‰ and +0.92‰, within the range of values for equilibrium partitioning at magmatic temperatures found in other Icelandic basalts (+0.65 ± 0.28‰: *Eiler et al., 2000*; +0.58 ± 0.24‰: *Thirlwall et al., 2006*). Three clinopyroxene-olivine pairs gave $\Delta^{18}O_{cpx-ol}$ values between +0.29‰ and +0.35‰, similar to values measured on Reykjanes Ridge samples (+0.28 ± 0.08‰: *Thirlwall et al., 2006*), while the ankaramite sample from Hvammsmuli gave a higher $\Delta^{18}O_{cpx-ol}$ value of +0.53‰. Olivines from the Snæfellsnes flank zone and from Heimaey and Hvammsmuli have oxygen isotope compositions of +4.7‰ to +5.1‰, which are consistent with the values measured by *Kokfelt et al. (2006)*, although their data range to slightly heavier values (+4.7‰ to +5.4‰). This range in $\delta^{18}O_{olivine}$ overlaps with that expected for mantle olivine (5.2 ± 0.3 ‰: *Mattey et al., 1994*), but includes some samples with lower values. Olivines from Snæfell have distinctly lower and relatively homogeneous $\delta^{18}O_{olivine}$ values (+4.4 ± 0.2‰: n = 7).

5. DISCUSSION

5.1 Crustal contamination processes

It is necessary to consider whether the Pb and He isotope compositions of the flank zone primitive lavas represent primary mantle source features or are modified by assimilation of crustal material. Crustal assimilation is difficult to recognise and quantify in an environment like

Iceland because of the limited compositional contrast between the mantle-derived magmas and the young mafic crust. The crust is not old enough (<15 Ma) for radioactive decay to significantly modify the isotopic composition of radiogenic elements such as Sr, Nd, Hf and Pb. Decay of U and Th in the crustal rocks can potentially create a reservoir of radiogenic ^{4}He with a composition distinct from that of mantle-derived melts (R/R_A ~0.05: e.g. *Condomines et al., 1983*). However, most mantle melts have relatively high helium concentrations, so the importance of crustal contamination depends on the extent to which the melt degasses helium during ascent through the crust, and it is notable that radiogenic helium ($^{3}He/^{4}He < 1\ R/R_A$) has never been observed in Icelandic basalts. The high latitude location of Iceland means that meteoric waters have very light $\delta^{18}O$ compositions, and interaction of crustal rocks with these waters through extensive hydrothermal systems leads to a shift in oxygen isotope composition to significantly lighter values than are typically found in mantle-derived melts (e.g. *Thirlwall et al., 2006; Bindeman et al., 2008*). Variations in $\delta^{18}O$, $^{3}He/^{4}He$ and $^{87}Sr/^{86}Sr$ with differentiation indices provide good evidence of crustal assimilation in evolved basalts to rhyolites, with examples known from the Northern Volcanic Zone (*Nicholson et al., 1991*) and the Eastern Volcanic Zone (*Bindeman et al., 2008*). The potential for crustal assimilation to modify magma compositions is likely to be greater for the flank zone lavas, as they are generally erupted through older and thicker crust compared to the rift zone lavas.

Crustal assimilation is expected to have a limited effect on the Pb isotope compositions of the erupted lavas on Iceland. Hydrothermal systems will largely redistribute Pb within the crust that is ultimately of mantle origin, and therefore the Icelandic crust should have a Pb isotope composition that lies within the observed data array of the lavas. Minor assimilation of local crustal rocks by a magma will just cause a small shift in its Pb isotope composition but it will still be within the main array. The general robustness of the Pb isotope system to the effects of crustal assimilation is highlighted by a suite of basaltic to rhyolitic lavas from the Torfajökull central volcano in the Eastern Volcanic Zone (*Stecher et al., 1999)*. The rhyolites have lower whole rock $\delta^{18}O$ values (+3.8 to +4.1‰: *Gunnarsson et al., 1998*) than the basalts (+4.9‰), indicative either of minor assimilation or an origin via melting of basaltic crust altered by meteoric waters (e.g. *Martin & Sigmarsson, 2007*). Irrespective of the actual model by which the rhyolites are generated, high precision Pb isotope data (*Baker et al., 2004*) show that the rhyolites plot in middle of the linear array defined by the basalts (Fig. 7a).

Öræfajökull provides a unique situation where there is a clear contrast between the anomalous high Δ^{207}Pb and Δ^{208}Pb compositions of the young flank-zone lavas and the normal Icelandic-type compositions of the older (~10-12 Ma) basement crust. This observation allowed *Prestvik et al. (2001)* to conclude that the anomalous compositions of Öræfajökull lavas were not the result of assimilation of local basement, but the question remains as to whether the trends shown on Pb isotope diagrams reflect assimilation between a high Δ^{207}Pb and Δ^{208}Pb mantle-derived melt and the local basement. The basalt to hawaiite lavas at Öræfajökull (3.5-6.1 wt% MgO) span a range in ^{206}Pb/^{204}Pb from 18.48 to 18.65 with little variation in whole rock δ^{18}O values (+5.3±0.2‰, 1 s.d.: *Prestvik et al., 2001*). The Öræfajökull mugearites to rhyolites (< 3.0 wt% MgO) plot slightly below the array for the more mafic samples, at lower Δ^{207}Pb, consistent with minor input from the local basement (Fig. 7b).

Four out of the five samples analysed from the Snæfellsnes flank zone, have a limited range in He and O isotope compositions, with ^{3}He/^{4}He values of 7.9 to 8.6 R/R$_A$ and $\delta^{18}O_{olivine}$ values of +4.9 to +5.1‰ that overlap with the typical range of mantle olivines (+5.2±0.3‰: *Mattey et al., 1994*). Sample 408765 from the Budahraun flow has lower $\delta^{18}O_{olivine}$ (+4.7‰) and lower ^{3}He/^{4}He (6.3 R/R$_A$), and *Kokfelt et al. (2006)* also showed that the Budahraun flow has lighter $\delta^{18}O_{olivine}$ (+4.8‰) compared to the other Snæfellsnes lavas in their study (+5.1 to +5.4‰). It is most likely that this reflects minor assimilation of altered crust in the Budahraun flow. This sample has the lowest MgO of the five studied Snæfellsnes samples (7.5 wt% vs. > 10 wt%) and the lowest He concentration (1.95 x 10^{-9} cc STP/g by crushing), and it also has anomalously low Cs/Rb (~ 0.007 vs. 0.011 for primitive mantle: *McDonough & Sun, 1995*), which *Chauvel & Hémond (2000)* suggested might be a tracer for shallow altered crust. In the Vestmannaeyjar flank zone, the one sample from Heimaey analysed for $\delta^{18}O_{olivine}$ gave a value of +5.0‰, which is the same as found by *Kokfelt et al. (2006)*, and it overlaps the expected range for typical mantle-derived melts. The Heimaey samples also show a constant He isotope composition (13.1-14.5 R/R$_A$) over a wide range in He concentrations (Fig. 5a), which suggests that these represent primary mantle features.

Snæfell lavas show a range in ^{206}Pb/^{204}Pb from 18.43 to 18.63, and there are small but distinct variations in incompatible trace element ratios that correlate with ^{206}Pb/^{204}Pb. Overall incompatible element enrichment is lower in the low ^{206}Pb/^{204}Pb samples (e.g. Zr/Y 6.4 vs. 6.9) that also have greater depletions of fluid mobile elements such as Cs and Rb (e.g. Cs/Nb 0.007

vs. 0.009; Rb/Nb 0.65 vs. 0.75). All of the Snæfell lavas have lighter $\delta^{18}O_{olivine}$ values (+4.1 to +4.6‰) than the other flank zone lavas and typical mantle olivines, which raises the issue of whether crustal assimilation is responsible. However, these samples show constant $^{3}He/^{4}He$ values (6.9-7.5 R/R_A: Fig. 5a) over a wide range in He concentrations, consistent with magma degassing, and the variations in $\delta^{18}O_{olivine}$ show no relationship to the variations in fluid mobile elements. Therefore, the low $\delta^{18}O$ and MORB-like $^{3}He/^{4}He$ of the Snæfell lavas are potentially inherited features from the mantle source. *Macpherson et al. (2005)* also demonstrated that some incompatible trace element enriched lavas (with $La/Sm_N > 2$ and $^{143}Nd/^{144}Nd$ ~0.51300) from the southern end of the Northern Volcanic Zone came from a mantle source with low $\delta^{18}O$ and MORB-like $^{3}He/^{4}He$.

5.2 Helium isotope composition of the trace element enriched end-members

Previous studies have noted the presence of two long-term trace element enriched mantle end-members in Iceland (Fig. 6a) as well as the broader North Atlantic region (e.g. *Mertz & Haase, 1997*): a *radiogenic-Sr* end member (intermediate $^{206}Pb/^{204}Pb$ and high $^{87}Sr/^{86}Sr$) and a *radiogenic-Pb* end member (high $^{206}Pb/^{204}Pb$ and intermediate $^{87}Sr/^{86}Sr$). Snæfell and Öræfajökull are representative of the radiogenic-Sr end member, and lavas from both places have MORB-like $^{3}He/^{4}He$ compositions (6.9-7.5 R/R_A: *Table 3; Sigmarsson et al., 1992*). Snæfellsnes and Vestmannaeyjar lavas have radiogenic Pb isotope compositions ($^{206}Pb/^{204}Pb$ >18.8) and, while Snæfellsnes lavas also have MORB-like $^{3}He/^{4}He$ values (7.5-8.6 R/R_A: *Table 3; Sigmarsson et al., 1992*), the Vestmannaeyjar lavas have elevated values (11.0-15.1 R/R_A: *Table 3; Kurz et al., 1985; Poreda et al., 1986; Debaille et al., 2009*), albeit nowhere near as high as the most extreme values yet found on Iceland (34-43 R/R_A: *Hilton et al., 1999; Breddam & Kurz, 2001; Macpherson et al., 2005*). However, the Vestmannaeyjar lavas have less enriched compositions than the Snæfellsnes lavas in terms of higher $^{143}Nd/^{144}Nd$ (Fig. 5b) and lower La/Sm_N. Samples with the highest $^{3}He/^{4}He$ values on Iceland also have higher $^{143}Nd/^{144}Nd$ than the Snæfellsnes lavas: Vadalda at the southern end of the Northern Volcanic Zone has $^{3}He/^{4}He$ of 34 R/R_A and $^{143}Nd/^{144}Nd$ of 0.51299 (*Macpherson et al., 2005*), and Seladalur in the Tertiary lavas of NW Iceland has $^{3}He/^{4}He$ of 38-43 R/R_A and $^{143}Nd/^{144}Nd$ of 0.51297 (*Hilton et al., 1999; Breddam & Kurz, 2001*). Lavas on Jan Mayen island, to the north of Iceland, sample an enriched mantle component with low $^{143}Nd/^{144}Nd$ ~0.51285 and intermediate $^{206}Pb/^{204}Pb$ ~18.54-18.71

(*Trønnes et al., 1999*) that also has low $^3He/^4He$ values (6.3-6.8 R/R_A: *Kurz et al., 1982*). Therefore, the most enriched components in the North Atlantic mantle are not the carriers of the high $^3He/^4He$ values (> 15 R/R_A) found in some lavas on Iceland and the adjacent ridges.

This is consistent with the trends shown by *Ellam & Stuart (2004)* for the older 47-62 Ma flood basalts of Greenland and Baffin Island that are generally thought to have formed from the initial stages of the ancestral Iceland hot spot. These samples generally form a positive correlation between $^3He/^4He$ and $^{143}Nd/^{144}Nd$, which suggest mixing between an 'enriched' end-member with $^{143}Nd/^{144}Nd < 0.5128$ and MORB-like $^3He/^4He$ and a 'depleted' end-member with $^{143}Nd/^{144}Nd > 0.5130$ and $^3He/^4He > 50$ R/R_A (Fig. 5b). Some of the older samples, as well as most recent Icelandic lavas are displaced away from this array towards the DMM (depleted MORB mantle) field with $^{143}Nd/^{144}Nd$ of 0.5130-0.5132 and $^3He/^4He$ ~8 R/R_A. The association of high $^3He/^4He$ with depleted mantle compositions, both within the North Atlantic region (e.g. *Ellam & Stuart, 2004 Macpherson et al., 2005*) and globally (e.g. *Kurz et al., 1982; Class & Goldstein, 2005*), can be explained by a variety of models that do not necessarily require the existence of a separate primordial mantle reservoir today. For example, experimental data indicate that He might be more compatible than U and Th during melting (e.g. *Parman et al., 2005*) which could allow development of high $^3He/^4He$ in depleted residues of melting, while *Albarède (2008)* suggests that high $^3He/^4He$ and solar neon diffused from primordial material into residual refractory mantle (dunites and harzburgites) with low U and Th contents early in Earth's history. However, these explanations might not be necessary as *Caro & Bourdon (in press)* have recently suggested that the Earth accreted with a super-chondritic Sm/Nd ratio, and they note that the high $^3He/^4He$ samples associated with the Iceland plume have $^{143}Nd/^{144}Nd$ values consistent with their revised value for the primitive mantle ($^{143}Nd/^{144}Nd$ ~0.51299). The low $^3He/^4He$ of the most enriched components in the Icelandic mantle are consistent with the presence of degassed, recycled material. Recycled oceanic crust is expected to have radiogenic $^3He/^4He$ (<1 R/R_A) due to high U and low ^3He (*Hanyu & Kaneoka, 1997*), but if the whole oceanic lithosphere is recycled, then the combined package (crust plus mantle) will evolve in 1-2 Ga to values only slightly more radiogenic (i.e. 6-7 R/R_A) than average MORB mantle (*Moreira & Kurz, 2001*).

5.3 EM-type components (= radiogenic-Sr end member)

Öræfajökull lavas are renowned within Iceland for having distinctly anomalous Sr-Pb

isotopic compositions that are found in the full compositional range from basalt to rhyolite (*Sigmarsson et al., 1992; Prestvik et al., 2001; Kokfelt et al., 2006*). They have higher $^{87}Sr/^{86}Sr$ (0.7036-0.7038) than any other Icelandic lavas (Fig. 6a), and plot clearly above the main Iceland array on Pb isotope diagrams to higher $^{207}Pb/^{204}Pb$ and $^{208}Pb/^{204}Pb$: i.e. high $\Delta^{207}Pb$ and $\Delta^{208}Pb$ (Fig. 4). These characteristics are consistent with the involvement of an 'Enriched Mantle' or EM-type mantle component as defined by *Zindler & Hart (1986)*. High-precision Pb isotope data show that high $\Delta^{207}Pb$ values are not unique to Öræfajökull. Snæfell lavas have elevated $\Delta^{207}Pb$ values relative to the majority of Icelandic lavas, albeit not to the same extent as at Öræfajökull (Fig. 4), and *Thirlwall et al. (2004)* and *Peate et al. (2009)* have demonstrated similar features in some Reykjanes Peninsula lavas. However, unlike the Snæfell and Öræfajökull samples, high $\Delta^{207}Pb$ values on the Reykjanes Peninsula are only found in some of the incompatible trace element depleted samples, and the most extreme example (sample RP103A: *Thirlwall et al., 2004*) has the lowest measured Nb/Zr (0.011) of any Icelandic lava and yet has relatively low $^{143}Nd/^{144}Nd$ (Fig. 2). *Thirlwall et al (2004)* argued that this discrepancy could be explained if the depleted, high $\Delta^{207}Pb$ Reykjanes Peninsula samples were derived from the residue from a relatively recent melting event of the enriched EM mantle source.

The origin of the EM-type signature at Iceland remains enigmatic. One issue is whether it has more of an EM1-type flavour (with unradiogenic $^{206}Pb/^{204}Pb$: e.g. *Sigmarsson et al., 1992; Hanan & Schilling, 1997; Thirlwall et al., 2004*) or an EM2-type flavour (with intermediate $^{206}Pb/^{204}Pb$: e.g. *Prestvik et al., 2001; Kokfelt et al., 2006*). *Hanan & Schilling (1997)* showed that Pb isotope variations (analysed by conventional TIMS methods) of the older Tertiary Iceland lava sequences (2.3-15.7 Ma) required the involvement of three components (Fig. 8). From the trends of the data in samples from specific time periods and locations, they argued that the high $\Delta^{207}Pb$ and $\Delta^{208}Pb$ component ('E' on Fig. 8) had low $^{206}Pb/^{204}Pb$, similar to the EM1 mantle end member of *Zindler & Hart (1986)*, and a similar conclusion was reached by *Kitagawa et al. (2008)* from high-precision double-spike Pb isotope analyses of the Tertiary lavas in Eastern Iceland. *Kokfelt et al. (2006)*, on the other hand, proposed a model for Öræfajökull in which a mantle source with $^{206}Pb/^{204}Pb$ ~18.44 was polluted with recycled pelagic sediments with $^{206}Pb/^{204}Pb$ ~18.5-19.3 and high $\Delta^{207}Pb$ and $\Delta^{208}Pb$. However, the Pb isotope arrays for both Öræfajökull and Snæfell show increasing $\Delta^{207}Pb$ and $\Delta^{208}Pb$ with decreasing $^{206}Pb/^{204}Pb$ which suggest the addition of a low $^{206}Pb/^{204}Pb$ EM1-type component to a radiogenic Pb mantle with

$^{206}Pb/^{204}Pb$ > 18.8 (Fig. 7b). The unradiogenic nature of the high $\Delta^{207}Pb$ component is also illustrated by the fact the sample with the highest $\Delta^{207}Pb$ from the Reykjanes Peninsula (sample RP103A), also has the lowest $^{206}Pb/^{204}Pb$ (Fig. 4: *Thirlwall et al., 2004*). The potential involvement of pelagic sediment material is also limited by the mantle-like (or even lower) $\delta^{18}O$ compositions of all Icelandic lavas (e.g. Fig. 6c). Pelagic sediments are also distinguished by having Hf isotope compositions that plot above the mantle array at low εNd on a Hf-Nd isotope plot (e.g. *Chauvel et al., 2008*). Figure 6b shows that the Öræfajökull samples plot on the mantle array, overlapping with samples from Snæfellsnes, which is further evidence ruling out a significant role for pelagic sediments in the origin of the Öræfajökull EM-type signature. However, *Kitagawa et al. (2008)* found that Tertiary Iceland lavas with the highest proportion of the high $\Delta^{207}Pb$ component also had higher εHf for a given εNd and plot above the mantle array (see Fig. 6b).

Models to explain the compositional features of EM1-type mantle include recycled ocean crust plus pelagic sediment, recycled oceanic plateaus, delaminated subcontinental lithosphere, and delaminated lower continental crust (e.g. *Hofmann, 1997; Gasperini et al., 2000; Hanan et al., 2004*). These degassed components are all expected to have low $^{3}He/^{4}He$ compositions similar to, or lower than, typical MORB values (e.g. *Hanyu & Kaneoka, 1997; Moreira & Kurz, 2001; Gautheron & Moreira, 2002*), consistent with what is observed at both Öræfajökull and Snæfell. *Hanan & Schilling (1997)* suggested that the EM1-type material represents entrained fragments of subcontinental lithospheric mantle embedded in the North Atlantic asthenosphere after delamination during initial continental break-up at ~55 Ma, and *Kitagawa et al. (2008)* proposed a similar model but involving delaminated lower continental crust (after *Hanan et al., 2004*). Either model would be consistent with the apparent variability in the Hf isotope characteristics of the high $\Delta^{207}Pb$ component in Iceland, as data suggests significant and variable decoupling of Nd and Hf isotopes in continental lithospheric mantle and granulitic lower crust (e.g. *Pearson et al., 2003; Schmitz et al., 2004*). An intriguing possibility raised by *Sigmarsson & Steinthorsson (2007)* is that the EM1-component is contributed by a fragment of continental lithosphere that was stranded beneath Eastern Iceland following the initial opening of the North Atlantic Ocean. This has been suggested from plate reconstructions (e.g. *Foulger & Anderson, 2005*) and from the presence of old zircons, based on reports in a couple of abstracts (*Schaltegger et al., 2002; Paquette et al., 2006*). Furthermore, in the study of *Hanan & Schilling (1997)*, lavas

from Eastern Iceland consistently showed a greater influence from the EM1-type component than lavas from Western Iceland during the same time interval. However, *Thirlwall et al. (2004),* instead, suggested that the EM1-type material (their ID2 component) was intrinsic to the Iceland plume upwelling as it did not appear to contribute to the magmatism on the surrounding mid-ocean ridges, and it is notable that the EM1-type component was also not a significant contributor to the magmatism that accompanied continental break-up in the North Atlantic region, as high-precision Pb isotope data on the Palaeogene East Greenland flood basalts all have negative Δ^{207}Pb (*Barker et al., 2006*).

5.4 High ^{206}Pb/^{204}Pb components (= radiogenic-Pb end member)

Post-glacial lavas with high ^{206}Pb/^{204}Pb (> 19.0) are only found in the Eastern Volcanic Zone (including Vestmannaeyjar) and in the Snæfellsnes flank zone (*Furman et al., 1991, 1995; Stecher et al., 1999; Thirlwall et al., 2004; this study*). As noted by *Chauvel & Hémond (2000)* and *Kokfelt et al. (2006)*, these high ^{206}Pb/^{204}Pb alkalic lavas have trace element characteristics such as elevated Ce/Pb and Nb/La and low K/Nb that are similar to HIMU-type basalts, which these authors attribute to recycled basaltic oceanic crust. However, they do not have the extreme radiogenic ^{206}Pb/^{204}Pb values that typify normal HIMU basalts (i.e. < 19.3 vs. > 20–22) which might suggest a younger age for the recycled material. The negative Δ^{207}Pb of this component (as well as the majority of Icelandic lavas) can be explained by evolution in a high-μ (μ=10–20, where μ is ^{238}U/^{204}Pb) source for less than 400 Ma (e.g. *Thirlwall et al., 2004*). *Blichert-Toft et al. (2005)* showed that HIMU material was also not necessary to explain the trend of Pb isotope compositions of North Atlantic MORB to the north and south of Iceland as it did not project through the field of global HIMU ocean islands. The Pb-Nd-Hf isotope compositions of the high ^{206}Pb/^{204}Pb (>19.0) Icelandic flank zone lavas overlap with the broad values that define the C or FOZO end-member (Fig. 6b) that is common to many MORB and OIB radiogenic isotope arrays (*Hanan & Graham, 1996; Stracke et al., 2005*), including North Atlantic MORB (*Blichert-Toft et al., 2005*). Snæfellsnes flank zone lavas have low ^{187}Os/^{188}Os values (0.127-0.130: *Smit et al., 2000; Debaille et al., 2009*), which appears to be typical for the FOZO/C end-member (*van Keken et al., 2002*). This relatively low ^{187}Os/^{188}Os can be explained in several ways: the amount of recycled basaltic crust is small; the recycled basaltic crust is young enough not to have developed a radiogenic ^{187}Os/^{188}Os signature; or any contribution of radiogenic Os from recycled basaltic crust is swamped by unradiogenic Os derived, together with MgO and Ni (e.g. *Chauvel*

& Hémond, 2000), from the host peridotitic mantle. Alternatively, the FOZO/C material may instead represent recycling of mantle wedge peridotite that was metasomatized by melts and fluids at subduction zones (e.g. *Donnelly et al., 2004*). Although some studies associate the FOZO/C component with a high $^{3}He/^{4}He$ signature (e.g. *Hart et al., 1992; van Keken et al., 2002*), the original study of *Hanan & Graham (1996)* showed that oceanic samples with Pb isotope compositions similar to FOZO/C can in fact have quite variable $^{3}He/^{4}He$, with values both higher than and lower than typical MORB values, and *Cadoux et al (2007)* showed that volcanics in Southern Italy with FOZO/C Pb isotope compositions had MORB-like $^{3}He/^{4}He$. Therefore, the low $^{3}He/^{4}He$ found in the Snæfellsnes flank zone lavas (6.3-8.6 R/R_A) are not unusual, and demonstrate that FOZO-like isotopic compositions are not universally associated with high $^{3}He/^{4}He$.

Thirlwall et al. (2006) inferred from a detailed study of oxygen isotope variations in lavas from the main rift zones that the enriched mantle components in Iceland should have light $\delta^{18}O_{olivine}$ values of <+4.6‰. This appears to be true for the EM-type component at Snæfell (+4.1 to +4.6‰), and *Macpherson et al. (2005)* also showed that incompatible trace element enriched basalts from the southern part of the Northern Volcanic Zone in central Iceland were derived from a mantle source with a lower oxygen isotope composition than normal mantle. However, our data together with those of *Kokfelt et al. (2006)* show that most of the high $^{206}Pb/^{204}Pb$ samples from both Snæfellsnes and Vestmannaeyjar have $\delta^{18}O_{olivine}$ values (Fig. 6c) that overlap with those expected for mantle olivine (5.18 ± 0.28 ‰: *Mattey et al., 1994*). These mantle-like values are consistent with previous conventional whole rock oxygen isotope measurements by *Sigmarsson et al. (1992)* and *Hémond et al. (1993)*. These data imply that the IE1 component of *Thirlwall et al. (2004)*, with $^{206}Pb/^{204}Pb$ ~19.35, in fact has normal mantle $\delta^{18}O$ values.

In detail, there are minor trace element and isotopic differences between the radiogenic Pb samples from the Eastern Volcanic Zone (including Vestmannaeyjar) and the Snæfellsnes flank zone. For example, they form different trends on $^{206}Pb/^{204}Pb$-$^{143}Nd/^{144}Nd$ and $^{206}Pb/^{204}Pb$-$^{87}Sr/^{86}Sr$ (Fig. 6a) isotope plots. At lower $^{206}Pb/^{204}Pb$ values (~18.9), the Snæfellsnes lavas have higher $^{87}Sr/^{86}Sr$ and lower $^{143}Nd/^{144}Nd$ than the Eastern Volcanic Zone lavas, while the trends converge at higher $^{206}Pb/^{204}Pb$ values (>19.3). However, they show contrasting characteristics in terms of Nd-Hf isotopes, as the Vestmannaeyjar plot on or below the mantle array on Fig. 6b ($\Delta\varepsilon_{Hf}$ -1.3 to 0.3), unlike all other Icelandic lavas, including those from Snæfellsnes ($\Delta\varepsilon_{Hf}$ 0.3 to

1.8), that plot above the mantle array ($\Delta\varepsilon_{Hf}$ is the vertical deviation of a sample from the mantle array on Fig. 6b). Some trace element differences such as the higher La/Yb_N of the Snæfellsnes lavas compared to those from the Eastern Volcanic Zone (Fig. 2a) most likely reflect different conditions of melt generation beneath these tectonically different regions. However, the lower La/Nb and K/Nb and higher Ce/Pb of the Snæfellsnes lavas, coupled with the difference in Nd-Hf isotopes, suggest that the mantle sources must also differ in composition. Therefore, there are small regional variations in the composition of the radiogenic Pb component in the Icelandic mantle between the Eastern Volcanic Zone and the Snæfellsnes flank zone in the west.

Older magmatism in Iceland and in the broader North Atlantic region also shows an influence from a radiogenic Pb component that is more similar to the composition of post-glacial lavas from the Eastern Volcanic Zone. For the older Tertiary (2-13 Ma) lava sequences of eastern Iceland, *Kitagawa et al. (2008)* showed from trends within the data that the mantle end-member with radiogenic Pb ($^{206}Pb/^{204}Pb$ ~19.5) also had negative $\Delta\varepsilon_{Hf}$ (~–2.8), similar to the Vestmannaeyjar lavas. Pb isotope data on the East Greenland and Faroe Islands flood basalts (*Holm et al., 2001; Peate & Stecher, 2003; Peate et al., 2003; Barker et al., 2006*) show that the Iceland radiogenic Pb component was also a significant contributor to the magmatism that accompanied continental break-up in the North Atlantic at ~55 Ma. In detail, the flood basalt lavas with $^{206}Pb/^{204}Pb$ > 19.0 share more compositional features with lavas from the Eastern Volcanic Zone than the Snæfellsnes flank zone, such as Nd-Hf isotope compositions that plot below the mantle array (Fig. 6b: *Peate et al., 2003; Barker, 2006*) and elevated $^{3}He/^{4}He$ (12-19 R/R_A in primitive alkaline picrites of the Prinsen af Wales Bjerge Formation, East Greenland: *Peate et al., 2003*).

5.5 Spatial distribution of local mixing end-members in the Icelandic mantle

The isotopic diversity of Icelandic lavas highlights the extent and complexity of compositional heterogeneity within the underlying mantle. Important issues are determining the number of compositionally distinct components that are present, their compositions, and their spatial relationships. Principal Component Analysis can be used to determine the minimum number of end-members needed to explain the Pb isotopic variability of the Icelandic lavas. *Blichert-Toft et al. (2005)* and *Debaille et al. (2006)* have argued that including other isotope systems (e.g. $^{87}Sr/^{86}Sr$, $^{143}Nd/^{144}Nd$, $^{176}Hf/^{177}Hf$) in the Principal Component Analysis can introduce spurious additional components, largely resulting from hyperbolic mixing effects.

Therefore, we restrict our Principal Component Analysis to just the high-precision double-spike Pb isotope data from this study, *Thirlwall et al. (2004)*, *Baker et al. (2004, 2005)* and *Peate et al. (2009)*. Using the three Pb isotope ratios ($^{206}Pb/^{204}Pb$, $^{207}Pb/^{204}Pb$, $^{208}Pb/^{204}Pb$), the first two components account for >99.5% of the variance (component 1 - 95.99%; component 2 - 3.54%; component 3 - 0.47%). The low abundance of the ^{204}Pb isotope can introduce correlations between isotope ratios with ^{204}Pb as the denominator, and so *Debaille et al. (2006)* argued that ^{206}Pb-normalised ratios should be used for the Principal Component Analysis. In this case, the first two components now account for >99.9% of the variance (component 1 - 99.03%; component 2 - 0.95%; component 3 - 0.02%). The Principal Component Analysis produces only two significant components which implies that mixing between three end-members can potentially produce all the Pb isotope compositions of Icelandic lavas. Furthermore, the fact that the first principal component accounts for such a large proportion of the total variance indicates that the Pb isotope variations are dominated by binary mixing between two of the components, which is consistent with the broad linear trends of the Pb isotope data in Fig. 4.

Hanan & Schilling (1997) proposed that the Pb isotope variations of Icelandic lavas could be explained in terms of mixing between three globally defined end-member mantle components: D – depleted MORB source mantle; P – plume component, similar to the common or C mantle component (*Hanan & Graham, 1996*); E – EM-1 enriched mantle component (Fig. 8). *Kitagawa et al. (2008)* also used three end-member components (D, E-1, E-2: Fig. 8) with similar but less extreme compositions than those of *Hanan & Graham (1996)* to model the Pb isotope variability in 2-13 Ma lavas in Eastern Iceland. However, by including Sr and Nd isotope data, *Thirlwall et al. (2004)* proposed that the Sr-Nd-Pb isotope systematics of Icelandic lavas required four compositionally-distinct regional mantle components (ID1, ID2, IE1, IE2: Fig. 8), whose compositions were estimated from the most extreme compositions measured in the lavas and from hyperbolic mixing curves involving Sr and Nd isotopes.

The limited precision of conventional TIMS Pb isotope data allows the array defined by Icelandic lavas (excluding Öræfajökull) to be explained as a simple binary mixing trend (e.g. *Kokfelt et al., 2006*). However, subtle but significant shifts away from a single linear trend can be resolved using high precision double-spike Pb isotope data (e.g. *Thirlwall et al., 2004; Baker et al., 2004; Peate et al., 2009*), which is apparent from the kinked shape of the Iceland array on a $^{208}Pb/^{204}Pb$ vs. $^{206}Pb/^{204}Pb$ diagram (Fig. 4c). *Thirlwall et al. (2004)* noted that samples from

geographically-restricted locations show tight linear Pb isotope correlations that indicate binary mixing, but in most cases the trends are not consistent with simple mixing between two of the regional (e.g. *Thirlwall et al., 2004*) or global (e.g. *Hanan & Schilling, 1997*) end-members. Instead, the end-members to these local mixing arrays potentially represent well-blended mixtures of the regional or global end-members (pseudo-binary mixing: e.g. *Douglass & Schilling, 2000*). These local end-members are then mixed in different proportions either within the mantle source to the specific rift system or, more likely, during the melt extraction process (e.g. *Maclennan, 2008; Peate et al., 2009*). Details of how these local mixing end-members vary between the volcanic systems on Iceland can potentially provide information about the distribution and length scale of heterogeneities within the mantle. However, care must be taken to definitely establish for each individual rift system whether crustal assimilation has influenced the Pb isotope trends.

The samples discussed in this paper are essentially restricted to the post-glacial period, i.e. the last ~13,000 years. Some of the subglacial pillow glasses from the axial rift zones (samples from *Kurz et al., 1985* and *Breddam et al., 2000*) likely have slightly older ages (~15-100 ka), and Snæfell is considerably older (~0.3 Ma: *Guillou et al., 2010*). The age of Hvammsmuli is uncertain but it is probably > 0.5 Ma. Consideration of plate separation velocities (10 mm/yr: *Searle et al., 1998*) and plausible estimates of mantle upwelling velocities (10-70 mm/yr at depths <100 km: *Maclennan et al., 2001; Kokfelt et al., 2003*) means that mantle material is unlikely to have moved more than 1 km laterally or vertically during the post-glacial time interval (~5 km for the subglacial rift glasses). *Maclennan (2008)* argued, based on seismic data and the compositional differences between adjacent volcanic centres (e.g. *Furman et al., 1995*), that the melting zone that feeds individual eruptions is less than 100 km in lateral extent. Therefore, the radiogenic isotope compositions of the post-glacial lavas can be used to map out the spatial distribution of compositional heterogeneities in the mantle beneath Iceland, at least on the scale of the individual volcanic centres. The length scale of mantle heterogeneities must be less than the dimensions of the melting zone that feeds individual lavas, given the diversity of Pb isotope compositions recorded in olivine-hosted melt inclusions from individual eruptions (*Maclennan, 2008*). Therefore the isotopic composition of individual lavas represent an averaged sample of the heterogeneities present throughout the height and width of the mantle melting column. *Kokfelt et al. (2003)* argued that melting beneath the Snæfellsnes flank zone took place

over a ~20 km interval (70 to 50 km depth), while beneath the main rift zone in central Iceland melting occurred over a ~ 70 km interval (110 to 40 km depth).

An important feature of the Icelandic high-precision Pb isotope data is the different Pb isotope composition and trend shown by each of the main axial rift zones. The most unradiogenic Pb isotope compositions are found in the Northern Volcanic Zone, where samples have a range in $^{206}Pb/^{204}Pb$ of 17.92 to 18.50 (similar to the 17.90 to 18.38 range found by *Stracke et al., 2003*). The double-spike data of the present study and *Thirlwall et al. (2004)* form an array above the NHRL on the $^{208}Pb/^{204}Pb$ vs. $^{206}Pb/^{204}Pb$ diagram ($\Delta^{208}Pb$ of 20 to 31: Fig. 4c) but with a slope slightly less than the NHRL. The Pb isotope composition of lavas from the Reykjanes Peninsula, which represents the southwestern extension of the Western Volcanic Zone, has been documented in *Thirlwall et al. (2004)* and *Peate et al. (2009)*. These lavas have a range in $^{206}Pb/^{204}Pb$ of 18.29 to 18.97 (excluding the EM-rich sample RP103A: *Thirlwall et al., 2004*) and form a trend that is markedly oblique to the NHRL and with a much shallower slope than the Northern Volcanic Zone lavas. Within the axial rift zones of Iceland, volcanism occurs at a series of individual volcanic systems that generally have a NNE to NE orientation (Fig. 1). Sample coverage of the axial rift zones is concentrated in a few locations, and so the contrasting Pb isotope compositions of the Northern Volcanic Zone and the Western Volcanic Zone are primarily defined by samples from the Theistareykir volcanic system for the Northern Volcanic Zone and the Reykjanes Peninsula for the Western Volcanic Zone. Ascertaining the location of the boundary between these contrasting compositional types, and whether the boundary is a sharp transition from one volcanic system to the next, is difficult to do at the present time due to the sparse sampling from central Iceland. The few samples analysed from the northern part of the Western Volcanic Zone in the Langjökull area have similar Pb isotope compositions to samples from the Reykjanes Peninsula. Of the two samples analysed from the next volcanic system to the east, one (SK82-05) is similar to the Reykjanes Peninsula samples, while the other (SK82-06) is similar to the Northern Volcanic Zone samples, and so the transition must lie somewhere in this region (Fig. 9a).

From the geometrical alignment of the volcanic systems, the Eastern Volcanic Zone represents the southern tectonic continuation of the Northern Volcanic Zone on the other side of the Vatnajökull ice cap. However, most lavas from the Eastern Volcanic Zone (Vestmannaeyjar, Torfajökull, Katla, Hekla) have radiogenic $^{206}Pb/^{204}Pb$ compositions of 18.92 to 19.30 that are

significantly higher than are found in any lavas from the Northern Volcanic Zone. Furthermore, these samples do not lie on an extension of the linear trend through the Northern Volcanic Zone lavas on a $^{208}Pb/^{204}Pb$ vs. $^{206}Pb/^{204}Pb$ plot (Fig. 9b), and instead form a sub-parallel linear array, displaced to lower $\Delta^{208}Pb$, similar to what *Abouchami et al. (2000)* found for Mauna Kea basalts on Hawaii. This requires that the local enriched mixing end-member for the Northern Volcanic Zone lavas is not related to the enriched mantle components beneath the Eastern Volcanic Zone and that there must be a significant compositional boundary within the mantle between these two rift systems despite their tectonic continuity.

Within the Eastern Volcanic Zone, there is a group of samples (e.g. Veidivötn, Laki/Grimsvötn) with significantly lower $^{206}Pb/^{204}Pb$ values (18.36 to 18.59: Table 2; *Chauvel & Hémond, 2000; Thirlwall et al., 2004; Kokfelt et al., 2006; Haldorsson et al., 2008*) that are more similar to the most radiogenic samples from the Northern Volcanic Zone (Fig. 9b: note that these samples are included with the Northern Volcanic Zone data on Fig. 9c and omitted from the Eastern Volcanic Zone data on Fig. 9d). This is not unsurprising as it has been shown that there has been significant lateral propagation (up to 100 km) of magma in these fissure systems from volcanic centres to the north-east beneath the Vatnajökull ice cap (e.g. *Sigmarsson et al., 2000*). Movement of magma along the strike of a volcanic system in this manner means that the location of compositional boundaries in the mantle are easier to delineate from a comparison of lava compositions from adjacent volcanic systems when the boundaries are oriented parallel to the volcanic systems. In contrast, even though there is a significant gap in Pb isotope composition of lavas moving south-west from the Northern Volcanic Zone into the Eastern Volcanic Zone along essentially a continuation of the same volcanic rift system (Fig. 9a), it is not possible to use the lava compositions to precisely locate where this boundary is, because of the lateral transfer of magma within each volcanic system. Furthermore, the lavas in the Veidivötn and Laki/Grimsvötn volcanic systems show evidence for extensive shallow level assimilation (e.g. *Bindeman et al., 2008*), and so their Pb isotope composition is likely to be strongly overprinted by the local basement composition. This may also be an important influence on the compositions of lavas elsewhere in the Northern Volcanic Zone, as illustrated in Fig. 9c ($\delta^{18}O_{olivine}$ vs. $^{206}Pb/^{204}Pb$). On this figure, lavas from the Theistareykir volcanic system in the north of the Northern Volcanic Zone (Fig. 9a) have unradiogenic Pb isotope compositions ($^{206}Pb/^{204}Pb$ 17.9-18.1) and $\delta^{18}O_{olivine}$ values of +4.2‰ to +4.9‰ lower than expected for normal mantle sources. The extent to which

these $\delta^{18}O_{olivine}$ values reflect crustal assimilation have been debated (e.g. *Eiler et al., 2000; Thirlwall et al. 2006*). Other lavas from the Northern Volcanic Zone, especially to the south of Theistareykir, have noticably higher $^{206}Pb/^{204}Pb$ compositions (18.2-18.5), and for these samples there is a broad trend towards lower $\delta^{18}O_{olivine}$ values (to < 3‰: Table 6) with increasing $^{206}Pb/^{204}Pb$ that is consistent with crustal assimilation. The lowest $\delta^{18}O_{olivine}$ values are found in lavas with Pb isotope compositions very similar to the average composition of eastern Iceland basaltic crust (calculated from the Pb isotope data of 2-13 Ma lavas from Eastern Iceland in *Kitagawa et al., 2008*).

A distinctive feature of the high-precision Pb isotope data for Icelandic lavas is the marked change in slope on the $^{208}Pb/^{204}Pb$ vs. $^{206}Pb/^{204}Pb$ diagram (Fig. 4c) at $^{206}Pb/^{204}Pb$ ~18.95. This feature was not resolved in the *Thirlwall et al. (2004)* study, as they only had a few samples with $^{206}Pb/^{204}Pb$ >19.0. This feature defines the relationship between the lava compositions of the Western Volcanic Zone and the Eastern Volcanic Zone (Fig. 9a). Samples from the Reykjanes Peninsula and elsewhere in the Western Volcanic Zone have $^{206}Pb/^{204}Pb$ values < 19.0 that form an oblique trend to the NHRL. The Eastern Volcanic Zone lavas (excluding those from the Veidivötn and Laki/Grimsvötn volcanic systems) have $^{206}Pb/^{204}Pb$ values > 18.9 that form a linear trend parallel to the NHRL (Fig. 4c, Fig. 9d) that converges at a common end-member with the most radiogenic samples from the Western Volcanic Zone. These samples are best represented by trace element enriched lavas from the Reykjanes Peninsula (*Thirlwall et al., 2004; Peate et al., 2009*). *Thirlwall et al. (2004)* suggested that this Enriched Reykjanes Peninsula end-member was a blend of their two enriched Icelandic components, IE1 and IE2, although *Thirlwall et al. (2006)* and *Peate et al. (2009)* argued that it has distinctly lower $\delta^{18}O_{olivine}$ values than inferred in this paper for the IE1 mantle component. In fact, the Enriched Reykjanes Peninsula end-member represents an important local mixing end-member in its own right that has a widespread distribution within the mantle of south-west Iceland.

A final issue is evaluating the possible relationship of the mantle sampled by the two flank zone (Snæfellsnes in the west, and Snæfell-Öræfajökull in the east) to that beneath the main axial rift zones. High precision Pb isotope data on the Snæfellsnes flank zone lavas overlap with the composition of lavas from the Eastern Volcanic Zone (Fig. 4). However, samples from the two areas show different trends on $^{87}Sr/^{86}Sr$-$^{206}Pb/^{204}Pb$ (Fig. 6a) and $^{143}Nd/^{144}Nd$-$^{206}Pb/^{204}Pb$ plots, with Snæfellsnes lavas having higher $^{87}Sr/^{86}Sr$ and lower $^{143}Nd/^{144}Nd$ than the Eastern Volcanic

Zone lavas at lower $^{206}Pb/^{204}Pb$ (~18.9). This indicates that the Enriched Reykjanes Peninsula component (with $^{206}Pb/^{204}Pb$ ~18.9) that is present in both the Western Volcanic Zone and the Eastern Volcanic Zone is not involved in the Snæfellsnes flank zone magmatism. Linear extrapolation of the trend of the Snæfellsnes Pb isotope data to lower $^{206}Pb/^{204}Pb$ requires any mixing end-member to have lower $\Delta^{208}Pb$ than other known Icelandic samples (Fig. 4d). One alternative is the possible involvement of a depleted component similar to that found on the Reykjanes Ridge as this has low $\Delta^{208}Pb$ of ~11 at $^{206}Pb/^{204}Pb$ of 18.2 (*Thirlwall et al., 2004*). However, using such a component would require a hyperbolic mixing curve to account for the trend of the Snæfellsnes lavas on the $^{87}Sr/^{86}Sr$-$^{206}Pb/^{204}Pb$ that can only be modelled with a Sr/Pb ratio much lower than expected for a depleted MORB source. It should be noted, though, that the closest part of the main axial rift system to the Snæfellsnes flank zone is the northern part of the Western Volcanic Zone, and we presently have very few high precision Pb isotope analyses for samples in this region. Trace element and Nd-Hf isotope data (Fig. 6b) indicate that the radiogenic Pb end-member (with $^{206}Pb/^{204}Pb$ > 19.3) at Snæfellsnes is also compositionally different to the radiogenic Pb end-member in the Eastern Volcanic Zone, and so it appears that neither of the local mixing end-member components beneath the Snæfellsnes flank zone noticeably contribute to the tholeiitic magmatism of the main axial rift zones. The Snæfell-Öræfajökull flank zone lies to the east of the Northern Volcanic Zone (Fig. 9a). Pb isotope trends (Fig. 4) for both Snæfell and Öræfajökull require that an EM-1-type end-member mixes with a radiogenic Pb end-member with $^{206}Pb/^{204}Pb$ at least > 18.7. This is higher than in any sample known from the Northern Volcanic Zone (max. $^{206}Pb/^{204}Pb$ = 18.51), although again the closest part of this axial rift zone to the Snæfell-Öræfajökull flank zone is a region for which we have few high-precision Pb isotope data. Within the axial rift zones, evidence for a contribution from the EM-1-type end-member has only been found in Reykjanes Peninsula part of the Western Volcanic Zone, far from the Snæfell-Öræfajökull flank zone, although it is known to have contributed to the earlier (2-13 Ma) magmatism of the Northern Volcanic Zone in the region of the current Snæfell-Öræfajökull flank zone (*Hanan & Schilling, 1997; Kitagawa et al., 2008*). Therefore, in detail, there does not appear to be a close relationship between the mantle end-member components beneath the flank zones and those beneath the main axial rift zones.

6. SUMMARY

Lavas in the flank zones of Iceland erupted through thicker and older crust and are more

alkaline in composition compared with the tholeiitic lavas of the main axial rift zones. High precision Pb isotope data show that samples from the Snæfell-Öræfajökull flank zone have anomalously high Δ^{207}Pb compared to other Icelandic lavas (except some from the Reykjanes Peninsula), and at Snæfell these EM-type features are accompanied by MORB-like ^{3}He/^{4}He. Lavas in the two other flank zones (Vestmannaeyjar / Eastern Volcanic Zone, Snæfellsnes) have radiogenic Pb isotope compositions (^{206}Pb/^{204}Pb >18.9) and a mantle-like oxygen isotope signature. In detail, there are differences between the two areas, with the Snæfellsnes lavas having higher La/Yb, lower εNd and lower ^{3}He/^{4}He than those from Vestmannaeyjar and the Eastern Volcanic Zone. However, the flank zone lavas all have ^{3}He/^{4}He values lower than 15 R/R_A, indicating that the compositionally enriched mantle components beneath Iceland represent degassed sources and are not the carriers of the high ^{3}He/^{4}He values that typify some Icelandic lavas and the adjacent ridges. Each of the main axial rift zones has a different Pb isotope composition and trend on a ^{208}Pb/^{204}Pb vs. ^{206}Pb/^{204}Pb diagram. This kinked array shown by the high precision Pb isotope data requires the involvement of more than two mixing end-member components in the mantle, in addition to the EM-type component. The Eastern and Western Volcanic Zones share a common local mixing end-member, while the Eastern and Northern Volcanic Zones define sub-parallel linear arrays. This demonstrates that there is a significant compositional heterogeneity between the mantle beneath north-east Iceland and south-west Iceland.

ACKNOWLEDGEMENTS This work was funded primarily by the Danish National Research Foundation through a grant to the former Danish Lithosphere Centre, with additional funding from the University of Iowa for the oxygen isotope analyses. The ICP-MS lab at Iowa was established through funding from NSF and the University of Iowa. We thank Kristján Jonasson and Solrun Bollingberg for invaluable field assistance, Tod Waight for help with the radiogenic isotope analyses, Joshua Curtice for help with the helium isotope analyses, and Jay Thompson for help with the ICP-MS analyses. David Peate acknowledges the Obermann Center for Advanced Studies at the University of Iowa for a Scholar appointment that allowed final preparation of the manuscript. Catherine Chauvel, Godfrey Fitton and Colin Macpherson are thanked for their official journal reviews.

REFERENCES

Abouchami, W., Galer, S.J.G. & Hofmann, A.W. (2000). High precision lead isotope systematics of lavas from the Hawaiian Scientific Drilling Project. *Chemical Geology* **169,** 187-209.

Albarède. F. (2008). Rogue mantle helium and neon. *Science* **319**, 943-945.

Anders, E. & Grevesse, N. (1989). Abundances of the elements: meteoric and solar. *Geochimica et Cosmochimica Acta* **53**, 197-214.

Andres, M., Blichert-Toft, J. & Schilling, J-G. (2004). Nature of the depleted upper mantle beneath the Atlantic: evidence from Hf isotopes in normal mid-ocean ridge basalts from 79°N to 55°S. *Earth and Planetary Science Letters* **225**, 89-103.

Baker, J.A., Peate, D.W., Waight, T.E. & Meyzen, C. (2004). Pb isotopic analysis of standards and samples using a ^{207}Pb-^{204}Pb double spike and thallium to correct for mass bias with a double-focussing MC-ICP-MS. *Chemical Geology* **211**, 275-303.

Baker, J.A., Peate, D.W., Waight, T.E. & Thirlwall, M. (2005). Reply to comment by Albarède et al. on "Pb isotopic analysis of standards and samples using a ^{207}Pb-^{204}Pb double spike and thallium to correct for mass bias with a double-focusing MC-ICP-MS". *Chemical Geology* **217**, 175-179.

Barker, A.K., Baker, J.A. & Peate, D.W. (2006). Interaction of the rifting East Greenland margin with a zoned ancestral Iceland plume. *Geology* **34**, 481-484.

Barker, A.K. (2006). Trace element and isotope constraints on mantle sources and processes in the North Atlantic and Cape Verde magmatism. Ph.D. thesis, University of Copenhagen, Denmark, 263 pp.

Bindeman, I.N., Gurenko, A., Sigmarsson, O. & Chaussidon, M. (2008). Oxygen isotope heterogeneity and disequilibria of olivine crystals in large volume Holocene basalts from Iceland: evidence for magmatic digestion and erosion of Pleistocene hyaloclastites. *Geochimica et Cosmochimica Acta* **72**, 4397-4420.

Blichert-Toft, J., Agranier, A., Andres, M., Kingsley, R., Schilling, J-G. & Albarède, F. (2005). Geochemical segmentation of the Mid-Atlantic Ridge north of Iceland and ridge–hot spot interaction in the North Atlantic. *Geochemistry, Geophysics, Geosystems* **6(1)**, Q01E19, doi:10.1029/2004GC000788.

Brandon, A.D., Graham, D.W., Waight, T.E. & Gautason, B. (2007). ^{186}Os and ^{187}Os enrichments and high-^{3}He/^{4}He sources in the Earth's mantle: evidence from Icelandic picrites. *Geochimica et Cosmochimica Acta* **71**, 4570-4591.

Breddam, K., Kurz, M.D. & Storey, M. (2000). Mapping out the conduit of the Iceland plume with helium isotopes. *Earth and Planetary Science Letters* **176**, 45-55.

Breddam, K. & Kurz, M.D. (2001). Helium isotope signatures of Icelandic alkaline lavas. *EOS (Transactions AGU)* **82**, F1315.

Breddam, K. (2002). Kistufell: primitive melt from the Iceland plume. *Journal of Petrology* **43**, 345-373.

Burnard, P. & Harrison, D. (2005). Argon isotope constraints on modification of oxygen isotopes in Iceland basalts by surficial processes. *Chemical Geology* **216**, 143-156.

Cadoux, A., Blichert-Toft, J., Pinti, D.L. & Albarède, F. (2007). A unique lower mantle source for Southern Italy volcanoes. *Earth and Planetary Science Letters* **259**, 227-238.

Caro, G. & Bourdon, B. (2010). Non-chondritic Sm/Nd ratio in the terrestrial planets: consequences for the geochemical evolution of the mantle-crust system. *Geochimica et Cosmochimica Acta*, in press.

Chauvel, C. & Hémond, C. (2000). Melting of a complete section of recycled oceanic crust: Trace element and Pb isotopic evidence from Iceland. *Geochemistry, Geophysics, Geosystems* **1**, doi:10.1029/1999GC000002.

Chauvel, C., Lewin, E., Carpentier, M., Arndt, N.T. & Marini, J.-C. (2008). Role of recycled oceanic basalt and sediment in generating the Hf-Nd mantle array. *Nature Geoscience* **1**, 64-67.

Class, C. & Goldstein, S.L. (2005). Evolution of helium isotopes in the Earth's mantle. *Nature* **436**, 1107-1112.

Condomines, M., Grönvold, K., Hooker, P.J., Muehlenbachs, K., O´Nions, R. K., Oskarsson, N., Oxburgh, E.R. (1983). Helium, oxygen, strontium, and neodymium isotopic relationships in Icelandic volcanics. *Earth and Planetary Science Letters* **66**, 125-136.

Debaille, V., Blichert-Toft, J., Agranier, A., Doucelance, R., Schiano, P. & Albarède, F. (2006). Geochemical component relationships in MORB from the Mid-Atlantic Ridge, 22-35°N. *Earth and Planetary Science Letters* 241, 844-862.

Debaille, V., Trønnes, R.G., Brandon, A.D., Waight, T.E., Graham, D.W. & Lee, C.-T.A. (2009). Primitive off-rift basalts from Iceland and Jan Mayen: Os-isotoic evidence for a mantle source containing enriched subcontinental lithosphere. *Geochimica et Cosmochimica Acta* 73, 3423-3449.

Dixon, E.T., Honda, M., McDougall, I., Campbell, I.H. & Sigurdsson, I. (2000). Preservation of near-solar neon isotope ratios in Icelandic basalts. *Earth and Planetary Science Letters* **180**, 309-324.

Donnelly, K.E., Goldstein, S.L., Langmuir, C.H. & Spiegelmann, M.M. (2004). Origin of enriched ocean ridge basalts and implications for mantle dynamics. *Earth and Planetary Science Letters* **226**, 347-366.

Douglass, J. & Schilling, J.-G. (2000). Systematics of three-component, pseudo-binary mixing lines in 2D isotope ratio space representations and implications for mantle plume – ridge interaction. *Chemical Geology* **163**, 1-23.

Eiler, J.M., Grönvold, K. & Kitchen, N (2000). Oxygen isotope evidence for the origin of chemical variations in lavas from Theistareykir volcano in Iceland's northern volcanic zone. *Earth and Planetary Science Letters* **184**, 269-286.

Eiler, J.M. (2001). Oxygen isotope variations of basaltic lavas and upper mantle rocks. *Reviews in Mineralogy and Geochemistry* **43**, 319-364.

Ellam, R.M. & Stuart, F.M. (2004). Coherent He-Nd-Sr isotope trends in high $^{3}He/^{4}He$ basalts: implications for a common reservoir, mantle heterogeneity and convection. *Earth and Planetary Science Letters* **228**, 511-523.

Eysteinsson, H. & Gunnarsson, K. (1995). Maps of gravity, bathymetry and magnetics for Iceland and surroundings, Orkustofnun, National Energy Authority, Geothermal Division, OS-95055/JHD-07.

Fitton, J.G., Saunders, A.D., Kempton, P.D. & Hardarson, B.S. (2003). Does depleted mantle form an intrinsic part of the Iceland plume? *Geochemistry, Geophysics, Geosystems* **4(3)**, 1032, doi:10.1029/2002GC0000424.

Foulger, G.R. & Anderson, D.L. (2005). A cool model for the Iceland hotspot. *Journal of Volcanology and Geothermal Research* **141**, 1-22.

Furman, T., Frey, F.A. & Park, K.-H. (1991). Chemical constraints on the petrogenesis of mildly alkaline lavas from Vestmannaeyjar, Iceland: the Eldfell (1973) and Surtsey (1963-1967) eruptions. *Contributions to Mineralogy and Petrology* **109**, 19-37.

Furman, T., Frey, F. A. & Park, K.-H. (1995). The scale of source heterogeneity beneath the Eastern neovolcanic zone, Iceland. *Journal of the Geological Society* **152**, 997-1002.

Gasparini, D., Blichert-Toft, J., Bosch, D., DelMoro, A., Macera, D., Télouk, P. & Albarède, F. (2000). Evidence from Sardinian basalt geochemistry for recycling of plume heads into the Earth's mantle. *Nature* **408**, 701-704.

Gebrande, H., Miller, H. & Einarsson, P. (1980). Seismic structure of Iceland along RRISP profile-1. *Journal of Geophysics* **47**, 239-249.

Gautheron, C.E. & Moreira, M. (2002). Helium signature of the subcontinental lithospheric mantle. *Earth and Planetary Science Letters* **199**, 39-47.

Guillou, H., Van Vliet-Lanoë, B., Gudmundsson, A. & Nomade, S. (2010). New unspiked K-Ar ages of Quaternary sub-glacial and sub-aerial volcanic activity in Iceland. *Quaternary Geochronology* 5, 10-19.

Graham, D.W. (2002). Noble gas isotope geochemistry of mid-ocean ridge and ocean island basalts:

characterization of mantle sources. *Reviews in Mineralogy and Geochemistry* **47**, 247-318.

Graham, D.W., Larsen, L.M., Hanan, B.B., Storey, M., Pedersen, A.K. & Lupton, J.E. (1998). Helium isotope composition of the early Iceland mantle plume inferred from the Tertiary picrites of West Greenland. *Earth and Planetary Science Letters* **160**, 241-255.

Gunnarsson, B., Marsh, B.D. & Taylor, H.P. (1998). Generation of Icelandic rhyolites: silicic lavas from the Torfajökull central volcano. *Journal of Volcanology and Geothermal Research* **83**, 1-45.

Haldorsson, S.A., Oskarsson, N., Grönvold, K., Sigurdsson, G., Sverrisdottir, G. & Steinthorsson, S. (2008). Isotopic heterogeneity of the Thjorsa lava – implications for mantle sources and crustal processes within the Eastern Rift Zone, Iceland. *Chemical Geology* **255,** 305-316.

Hanan, B.B. & Graham, D.W. (1996). Lead and helium isotope evidence from oceanic basalts for a common deep source of mantle plumes. *Science* **272**, 991-995.

Hanan, B.B. & Schilling, J.-G. (1997). The dynamic evolution of the Iceland mantle plume: the Pb isotope perspective. *Earth and Planetary Science Letters* **151**, 43-60.

Hanan, B.B., Blichert-Toft, J., Pyle, D.G. & Christie, D.M. (2004). Contrasting origins of the upper mantle revealed by hafnium and lead isotopes from the Southeast Indian Ridge. *Nature* **432,** 91-94.

Hanyu, T. & Kaneoka, I. (1997). The uniform and low $^{3}He/^{4}He$ ratios of HIMU basalts as evidence for their origin as recycled materials. *Nature* **390**, 273-276.

Hards, V.L., Kempton, P.D. & Thompson, R.N. (1995). The heterogeneous Iceland plume: new insights from the alkaline basalts of the Snaefell volcanic centre. *Journal of the Geological Society* **152**, 1003-1009.

Hards, V.L., Kempton, P.D., Thompson, R.N. & Greenwood, P.B. (2000). The magmatic evolution of the Snaefell volcanic centre: an example of volcanism during incipient rifting in Iceland. *Journal of Volcanology and Geothermal Research* **99**, 97-121.

Hart, S.R. (1984). A large-scale isotope anomaly in the southern hemisphere mantle. *Nature* **309**, 753-757.

Hart, S.R., Hauri, E.H., Oschmann, L.A. & Whitehead, J.A. (1992). Mantle plumes and entrainment: isotopic evidence. *Science* **256**, 517-520.

Hémond, C., Arndt, N.T., Lichtenstein, U. & Hofmann, A.W. (1993). The heterogeneous Iceland mantle plume: Nd-Sr-O isotopes and trace element constraints. *Journal of Geophysical Research* **98**, 15833-15850.

Hilton, D.R., Grönvold, K., O'Nions, R.K. & Oxburgh, E.R. (1990). Regional distribution of ^{3}He anomalies in the Icelandic crust. *Chemical Geology* **88**, 53-67.

Hilton, D.R., Grönvold, K., Macpherson, C.G., Castillo, P.R. (1999). Extreme $^{3}He/^{4}He$ ratios in northwest Iceland: constraining the common component in mantle plumes. *Earth and Planetary Science Letters* **173**, 53-60.

Hilton, D.R., Thirlwall, M.F., Taylor, R.N., Murton, B.J. & Nichols, A. (2000). Controls on degassing along the Reykjanes Ridge with implications for the helium paradox. *Earth and Planetary Science Letters* **183**, 43-50.

Hofmann, A.W. (1997). Mantle geochemistry: the message from oceanic volcanism. *Nature* **385**, 219-229.

Holm, P.M., Hald, N. & Waagstein, R. (2001). Geochemical and Pb-Sr-Nd isotopic evidence for separate hot depleted and Iceland plume mantle sources for the Paleogene basalts of the Faroe Islands. *Chemical Geology* **178**, 95-125.

Jakobsson, S.P. (1972). Chemistry and distribution pattern of Recent basaltic rocks in Iceland. *Lithos* **5**, 365-386.

Johannesson, H. & Saemundsson, K. (1998). Geological map of Iceland, 1:500,000, Tectonics, Icelandic

Institute of Natural History, Reykjavik.

Kempton, P.D., Fitton, J.G., Saunders, A.D., Nowell, G.M., Taylor, R.N., Hardarson, B.S. & Pearson, G. (2000). The Iceland plume in space and time: a Sr-Nd-Pb-Hf study of the North Atlantic rifted margin. *Earth and Planetary Science Letters* **177**, 255-271.

Kitagawa, H., Kobayashi, K., Makishima, A. & Nakamura, E. (2008). Multiple pulses of the mantle plume: evidence from Tertiary Icelandic lavas. *Journal of Petrology* **49**, 1365-1396.

Kokfelt, T.F., Hoernle, K. & Hauff, F. (2003). Upwelling and melting of the Iceland plume from radial variation of ^{238}U-^{230}Th disequilibria in postglacial volcanic rocks. *Earth and Planetary Science Letters* **214**, 167-186.

Kokfelt, T.F., Hoernle, K., Hauff, F., Fiebig, J., Werner, R. & Garbe-Schönberg, D. (2006). Combined trace element and Pb-Nd-Sr-O isotope evidence for recycled oceanic crust (upper and lower) in the Iceland mantle plume. *Journal of Petrology* **47**,1705-1749.

Kurz, M.D., Meyer, P.S. & Sigurdsson, H. (1985). Helium systematics within the neovolcanic zones of Iceland. *Earth and Planetary Science Letters* **74**, 271-305.

Kurz, M.D. (1986). In situ production of terrestrial cosmogenic helium and some applications to geochronology. *Geochimica et Cosmochimica Acta*, **50**, 2855-2862.

Kurz, M.D., Jenkins, W.J. & Hart, S.R. (1982). Helium isotopic systematics of oceanic islands and mantle heterogeneity. *Nature* **297**, 43-47.

Kurz, M.D. & Geist, D. (1999). Dynamics and evolution of the Galapagos hotspot from helium isotope geochemistry. *Geochimica et Cosmochimica Acta* **63**, 4139-4156.

Kystol, J. & Larsen, L.M. (1999). Analytical procedures in the rock geochemical laboratory of the Geological Survey of Denmark and Greenland. *Geology of Greenland Survey Bulletin* **184**, 59-62.

Le Maitre, R.W., Bateman, P., Dudek, A., Keller, J., Le Bas, M.J., Sabine, P.A., Schmid, R., Sørensen, H., Streckeisen, A., Woolley, A.R. & Zanettin, B. (1989) A classification of igneous rocks and glossary of terms. Blackwell, Oxford.

Luais, B., Telouk, P. & Albarède, F. (1997). Precise and accurate neodymium isotopic measurement by plasma source mass spectrometry. *Geochimica et Cosmochimica Acta* **61**, 4847-4854.

Maclennan, J., McKenzie, D.P. & Grönvold, K. (2001). Plume-driven upwelling under central Iceland. *Earth and Planetary Science Letters* **194**, 67-82.

Maclennan, J. (2008). Lead isotope variability in olivine-hosted melt inclusions from Iceland. *Geochimica et Cosmochimica Acta* **72**, 4159-4176.

Macpherson, C.G., Hilton, D.R., Day, J.M.D., Lowry, D. & Grönvold, K. (2005). High-^{3}He/^{4}He, depleted mantle and low-δ^{18}O, recycled oceanic lithosphere in the source of central Iceland magmatism. *Earth and Planetary Science Letters* **223**, 411-427.

Martin, E. & Sigmarsson, O. (2007). Crustal thermal state and origin of silicic magma in Iceland: the case of Torfajökull, Ljósufjöll, and Snæfellsjökull volcanoes. *Contributions to Mineralogy and Petrology* **153**, 593-605.

Marty, B., Upton, B.G.J. & Ellam, R.M. (1998). Helium isotopes in early Tertiary basalts, northeast Greenland: evidence for 58Ma plume activity in the North Atlantic – Iceland volcanic province. *Geology* **26**, 407-410.

Mattey, D.P. & Macpherson, C. (1993). High-precision oxygen isotope microanalysis of ferromagnesian minerals by laser fluorination. *Chemical Geology* **105**, 305-318.

Mattey, D.P., Lowry, D. & Macpherson, C. (1994). Oxygen isotope composition of mantle peridotite. *Earth and Planetary Science Letters* **128**, 231-241.

Mattsson, H.B. & Oskarsson, N. (2005). Petrogenesis of alkaline basalts at the tip of a propagating rift: evidence from the Heimey volcanic center, south Iceland. *Journal of Volcanology and Geothermal*

Research **147**, 245-267.

McDonough, W.F. & Sun, S.-s. (1995). The composition of the Earth. *Chemical Geology* **120,** 223-253.

Mertz, D.F. & Haase, K.M. (1997). The radiogenic isotope composition of the high-latitude North Atlantic mantle. *Geology* **25**, 411-414.

Moreira, M., Breddam, K., Curtice, J. & Kurz, M. D. (2001). Solar neon in the Icelandic mantle: new evidence for an undegassed lower mantle. *Earth and Planetary Science Letters* **185**, 15-23.

Moreira, M. & Kurz, M.D. (2001). Subducted oceanic lithosphere and the origin of the 'high μ' basalt helium isotopic signature. *Earth and Planetary Science Letters* **189**, 49-57.

Nicholson, H., Condomines, M., Fitton, J.G., Fallick, A.E., Grönvold, K & Rogers, G. (1991). Geochemical and isotopic evidence for crustal assimilation beneath Krafla, Iceland. *Journal of Petrology* **32**, 1005-1020.

Nielsen, S.G., Rehkämper, M., Brandon, A.D., Norman, M.D., Turner, S.P. & O'Reilly, S.Y. (2007). Thallium isotopes in Iceland and Azores lavas – implications for the role of altered crust and mantle geochemistry. *Earth and Planetary Science Letters* **264**, 332-345.

Oskarsson, N., Sigvaldson, G.E. & Steinthorsson, S. (1982). A dynamic model of rift zone petrogenesis and regional petrology of Iceland. *Journal of Petrology* **23**, 28-74.

Park, K.-H. (1990). Sr, Nd and Pb isotope studies of Ocean Island Basalts: constraints on their origin and evolution. Ph.D. dissertation, Columbia University, 252 pp.

Paquette, J.L., Sigmarsson, O. & Tiepolo, M. (2006). Continental basement beneath Iceland revealed by old zircons. *EOS (Transactions AGU)* **87(52)**, V33A-0642.

Parman, S.W., Kurz, M.D., Hart, S.R. & Grove, T.L. (2005). Helium solubility in olivine and implications for high $^{3}He/^{4}He$ in ocean island basalts. *Nature* **437**, 1140-1143.

Pearson, D.G., Canil, D. & Shirey, S.B. (2003). Mantle samples included in volcanic rocks: xenoliths and diamonds. *Treatise of Geochemistry* 2, 171-275.

Peate, D.W., Baker, J.A., Blichert-Toft, J., Hilton, D., Storey, M., Kent, A.J.R., Brooks, C.K., Hansen, H., Pedersen, A.K. & Duncan, R.A. (2003). The Prinsen af Wales Bjerge Formation lavas, East Greenland: the transition from tholeiitic to alkalic magmatism during Palaeogene continental break-up. *Journal of Petrology* **44**, 279-304.

Peate, D.W. & Stecher, O. (2003). Pb isotope evidence for contributions from different Iceland plume components to Palaeogene East Greenland flood basalts. *Lithos* **67**, 39-52.

Peate, D.W., Baker, J.A., Jakobsson, S.P., Waight, T.E., Kent, A.J.R. & Grassineau, N.V. (2009). Historic magmatism on the Reykjanes Peninsula, Iceland: a snap-shot of melt generation at a ridge segment. *Contributions to Mineralogy and Petrology* **157**, 359-382.

Poreda, R., Schilling, J.G. & Craig, H. (1986). Helium and hydrogen isotopes in ocean-ridge basalts north and south of Iceland. *Earth and Planetary Science Letters* **78**, 1-17.

Prestvik, T., Goldberg, S., Karlsson, H. & Grönvold, K. (2001). Anomalous strontium and lead isotope signatures in the off-rift Öræfajökull central volcano in south-east Iceland: evidence for enriched end-member(s) of the Iceland mantle plume? *Earth and Planetary Science Letters* **190**, 211-220.

Salters, V.J.M. & White, W.M. (1998). Hf isotope constraints on mantle evolution. *Chemical Geology* **145**, 447-460.

Schaltegger, U., Amundsen, H., Jamveit, B., Frank, M., Griffin, W.L., Grönvold, K., Trønnes, R. & Torsvik, T. (2002). Contamination of OIB by underlying ancient continental lithosphere: U-Pb and Hf isotopes in zircons question EM1 and EM2 mantle components. *Geochimica et Cosmochimica Acta* **66**, A673 (abstract).

Schilling, J.-G., Kingsley, R., Fontignie, D., Poreda, R. & Xue, S. (1999). Dispersion of the Jan Mayen and Iceland mantle plumes in the Arctic: a He-Pb-Nd-Sr isotope tracer study of basalts from the Kolbeinsey, Mohns and Knipovich Ridges. *Journal of Geophysical Research* **104**, 10543-10569.

Schmitz, M.D., Vervoort, J.D., Bowring, S.A. & Patchett, P.J. (2004). Decoupling of the Lu-Hf and Sm-Nd isotope systems during evolution of granulitic lower crust beneath southern Africa. *Geology* 32, 405-408.

Searle, R.C., Keeton, J.A., Owens, R.B., White, R.S., Mecklenburgh, R., Parson, B. & Lee, S.M. (1998). The Reykjanes Ridge: structure and tectonics of a hot-spot-influenced, slow-spreading ridge, from multibeam bathymetry, gravity and magnetic investigations. *Earth and Planetary Science Letters* **160**, 463-478.

Sigmarsson, O. Condomines, M. & Fourcarde, S. (1992). Mantle and crustal contribution in the genesis of Recent basalts from off-rift zones in Iceland: Constraints from Th, Sr and O isotopes. *Earth and Planetary Science Letters* **110**, 149-162.

Sigmarsson, O., Karlson, H.R. & Larsen, G. (2000). The 1996 and 1998 subglacial eruptions beneath the Vatnajökull ice sheet in Iceland: contrasting geochemical and geophysical inferences on magma migration. *Bulletin of Volcanology* **61**, 468-476.

Sigmarsson, O. & Steinthorsson, S. (2007). Origin of Icelandic basalts: a review of their petrology and geochemistry. *Journal of Geodynamics* **43**, 87-100.

Skovgaard, A.C., Storey, M., Baker, J.A., Blusztajn, J. & Hart, S.R. (2001). Osmium - oxygen isotopic evidence for a recycled and strongly depleted component in the Iceland mantle plume. *Earth and Planetary Science Letters* **194**, 259-275.

Smit, Y. (2001). The Snaefellsnes transect: a geochemical cross-section through the Iceland plume. Ph.D. thesis (unpublished), The Open University, Milton Keynes, UK, 241 pp.

Smit, Y., Parkinson, I.J., Peate, D.W., Hawkesworth, C.J. & Cohen, A.S. (2000). Osmium isotope characteristics of the Iceland plume. *EOS (Transactions, AGU)* **81**, F1344.

Stecher, O., Carlson, R.W. & Gunnarsson, B. (1999). Torfajökull: a radiogenic end-member of the Iceland Pb-isotopic array. *Earth and Planetary Science Letters* **165**, 117-127.

Steinthorsson, S., Oskarsson, N. & Sigvaldason, G.E. (1985). Origin of alkali basalts in Iceland: a plate tectonic model. *Journal of Geophysical Research* **90**, 10027-10042.

Steinthorsson, S. (1964) The ankaramites of Hvammsmuli, Eyjafjöll, southern Iceland. *Acta Naturalia Islandica* **2**, 1-32.

Stracke, A., Zindler, A., Salters, V.J.M., McKenzie, D., Blichert-Toft, J., Albarède, F. & Grönvold, K. (2003). Theistareykir revisited. *Geochemistry, Geophysics, Geosystems* **4(2)**, 8507, doi:10.1029/2001GC000201.

Stracke, A., Hofmann, A.W. & Hart, S.R. (2005). FOZO, HIMU, and the rest of the mantle zoo. *Geochemistry, Geophysics, Geosystems* **6(5)**, Q05007, doi:10.1029/2004GC000824.

Stuart, F.M., Lass-Evans, S., Fitton, J.G. & Ellam, R.M. (2003). Constraints on mantle plumes from the helium isotopic composition of basalts from the British Tertiary Igneous Province. *Earth and Planetary Science Letters* **177**, 273-285.

Stuart, F.M., Ellam, R.M., Harrop, P.J., Fitton, J.G. & Bell, B.R. (2000). High $^{3}He/^{4}He$ ratios in picritic basalts from Baffin Island and the role of mixed reservoirs in mantle plumes. *Nature* **424**, 57-59.

Thirlwall, M.F., Gee, M.A.M., Taylor, R.N. & Murton, B.J. (2004). Mantle components in Iceland and adjacent ridges investigated using double-spike Pb isotope ratios. *Geochimica et Cosmochimica Acta* **68**, 361-386.

Thirlwall, M.F., Gee, M.A.M., Lowry, D., Mattey, D.P., Murton, B.J. & Taylor, R.N. (2006). Low $\delta^{18}O$ in the Icelandic mantle and its origins: evidence from Reykjanes Ridge and Icelandic lavas. *Geochimica et Cosmochimica Acta* **70**, 993-1019.

Trønnes, R.G., Planke, S., Sundvoll, B. & Imsland, P. (1999). Recent volcanic rocks from Jan Mayen: low-degree melt fractions of enriched northeast Atlantic mantle. *Journal of Geophysical Research* **104**, 7153-7168.

Ulfbeck, D., Baker, J.A., Waight, T. & Krogstad, E. (2003). Rapid sample digestion by fusion and chemical separation of Hf for isotopic analysis by MC-ICP-MS. *Talanta* **59**, 365-373.

van Keken, P.E., Hauri, E.H. & Ballentine, C.J. (2002). Mantle mixing: the generation, preservation and destruction of chemical heterogeneity. *Annual Review of Earth and Planetary Sciences* **30**, 493-525.

Waight, T.E., Baker, J.A. & Peate, D.W. (2002). Sr isotope ratio measurements by double-focusing MC-ICP-MS: techniques, observations, and pitfalls. *International Journal of Mass Spectrometry* **221**, 229-244.

Wiese, P.K. (1992). Geochemistry and geochronology of the Eyjafjöll volcanic system, Iceland. M.Sc. thesis (unpublished), Oregon State University, USA, pp. 230.

Wolfe, C.J., Bjarnason, I.T., VanDecar, J.C. & Solomon, S.C. (1997). Seismic structure of the Iceland mantle plume. *Nature* **385**, 245-247.

Zindler, A. & Hart, S.R. (1997). Chemical geodynamics. *Annual Review of Earth and Planetary Sciences* **14**, 493-571.

FIGURE CAPTIONS

Figure 1 Map of Iceland showing the configuration of neo-volcanic rift zones outlined by volcanic systems (light shading: simplified from *Johannesson & Saemundsson, 1998*) and the main geophysical anomalies. The location of the three flank volcanic zones sampled in this study (Snæfell, Vestmannaejyar, Snæfellsnes) are highlighted, and the individual sample locations are shown by the filled circles (including the additional samples analysed for high precision Pb isotopes). WVZ, EVZ, NVZ: Western, Eastern and Northern Volcanic Zones, respectively. Bouguer gravity contours (in mGal) are from *Eysteinsson & Gunnarsson (1995)*. The thick stippled ellipse outlines the s-wave low velocity anomaly at 125 km depth that has been inferred to represent the axis of an upwelling plume beneath Iceland (*Wolfe et al., 1997*).

Figure 2 (a) La/Yb_N vs. Dy/Yb_N, (b) Nb/Zr vs. εNd, and (c) Nb/Zr vs. $^{206}Pb/^{204}Pb$. Chondrite-normalising values from *Anders & Grevesse (1989)*. Data sources for post-glacial Icelandic magmatism: *Chauvel & Hémond (2000); Breddam et al. (2000); Kempton et al. (2000); Hards et al. (2000); Smit (2001); Prestvik et al. (2001); Skovgaard et al. (2001); Stracke et al. (2003); Thirlwall et al. (2004); Macpherson et al. (2005); Mattson & Oskarsson, (2005); Kokfelt et al. (2006); Nielsen et al. (2007); Peate et al. (2009); Debaille et al. (2009).* Axial rift zone lavas are shown with an 'x' symbol in (a) and (b). Regional differences in Pb isotope composition of the axial rift zones are highlighted in (c) by plotting samples from the WVZ and the NVZ with different symbols.

Figure 3 (a) total alkalis - silica diagram (*Le Maitre et al., 1989*), (b) primitive-mantle-normalised trace element patterns of Icelandic lavas (normalising values from *McDonough & Sun, 1995*). Data source: same as for Figure 2.

Figure 4 Pb isotope variations in post-glacial Icelandic lavas. (a) $^{207}Pb/^{204}Pb$ vs. $^{206}Pb/^{204}Pb$, (b) $\Delta^{207}Pb$ vs. $^{206}Pb/^{204}Pb$, (c) $^{208}Pb/^{204}Pb$ vs. $^{206}Pb/^{204}Pb$, (d) $\Delta^{208}Pb$ vs. $^{206}Pb/^{204}Pb$. Plotted data are double-spike analyses from *Thirlwall et al. (2004); Peate et al. (2009), Waight (personal communication, 2007)*, and Table 3. $\Delta^{207}Pb$ and $\Delta^{208}Pb$ are the vertical deviations from the Northern Hemisphere Reference Line (after *Hart, 1984*).

Figure 5 (a) $^{3}He/^{4}He$ (R/R_A) versus helium concentration (x 10^{-9} cm^3 STP/g) for Icelandic lavas. Helium extraction from olivines is by crushing in vacuum and so helium concentrations are not total concentrations as they depend on the efficiency of the crushing process. Dotted line encloses data from olivines. Where two symbol sizes are used for samples from the same region (on this plot and subsequent figures), the large symbols are data from this study and the small symbols are published data. Data sources: *Condomines et al. (1983); Kurz et al. (1985); Poreda et al. (1986); Hilton et al. (1999); Dixon et al. (2000); Breddam et al. (2000); Burnard & Harrison (2005); Macpherson et al. (2005); Brandon et al. (2007); Debaille et al (2009)*. The range for MORB (8.75 ± 2.14: *Graham, 2002*) is shown by the dashed lines. Samples from Örafæjökull and Snæfellsnes in *Sigmarrson et al. (1992)* do not have accompanying He concentration data and they are plotted at an arbitrary value (highlighted by the arrow). (b) $^{3}He/^{4}He$ (R/R_A) vs. εNd for Icelandic lavas and the Paleogene magmatism of the North Atlantic Igneous Province. Data sources: Iceland (*Hilton et al., 1999; Breddam et al., 2000; Ellam & Stuart, 2004; Debaille et al., 2009*), Greenland and Baffin Island (*Graham et al. 1998; Marty et al., 1998; Stuart et al., 2000; Peate et al. 2003; Stuart et al. 2003*). DMM = 'depleted MORB mantle'.

Figure 6 (a) $^{87}Sr/^{86}Sr$ vs. $^{206}Pb/^{204}Pb$. Data sources: *Park (1990); Hards et al. (1995); Stecher et al., (1999); Chauvel & Hémond (2000); Breddam et al. (2000); Kempton et al. (2000); Prestvik et al. (2001); Stracke et al. (2003); Thirlwall et al. (2004); Baker et al. (2004); Kokfelt et al. (2006); Peate et al. (2009).* (b) εNd vs. εHf. Data sources: *Stracke et al. (2003); Blichert-Toft et al. (2005);* Table 4. Shaded field represents 2-

13 Ma rift zone lavas from eastern Iceland (*Kitagawa et al., 2008*). Line represents 'mantle array' (εHf = 1.4 εNd + 2.8) from *Andres et al. (2004)*. A = composition of end-member common to isotopic arrays for North Atlantic and Arctic MORB (*Blichert-Toft et al., 2005*). Shaded field with black dotted line represents estimated range for the 'C' mantle end-member of *Hanan & Graham (1996)* taken from *Blichert-Toft et al. (2005)*. (c) εNd vs. $\delta^{18}O_{olivine}$. Data sources: *Eiler et al. (2000); Kokfelt et al. (2006); Thirlwall et al. (2006); Peate et al. (2008)*. For some samples, $\delta^{18}O_{olivine}$ was calculated from $\delta^{18}O_{glass}$ assuming an olivine-melt fractionation factor of +0.4‰ (e.g. *Eiler, 2001*).

Figure 7 (a) $^{208}Pb/^{204}Pb$ vs. $^{206}Pb/^{204}Pb$ for Torfajökull lavas (high precision Pb isotope data from *Baker et al., 2004*; SiO_2 data from *Stecher et al., 1999*); (b) $\Delta^{207}Pb$ vs. $^{206}Pb/^{204}Pb$ for Örafæjökull lavas.

Figure 8 $^{206}Pb/^{204}Pb$ vs. $^{208}Pb/^{204}Pb$ plot showing the isotopic diversity of post-glacial Icelandic lavas in relation to the regional end-member mantle components proposed by *Hanan & Schilling (1997)* [D, P, E], *Thirlwall et al. (2004)* [ID1, ID2, IE1, IE2] and *Kitagawa et al. (2008)* [D, E-1, E-2].

Figure 9 **(a)** Location map outlining the compositional boundaries of mantle heterogeneity beneath Iceland as defined by high-precision Pb isotope data. (b) $^{206}Pb/^{204}Pb$ vs. $^{208}Pb/^{204}Pb$ diagram to illustrate the sub-parallel linear arrays defined by double-spike data on lavas from the Northern Volcanic Zone and the Eastern Volcanic Zone. (c) $^{206}Pb/^{204}Pb$ vs. $\delta^{18}O_{olivine}$ for the Northern Volcanic Zone lavas. Data sources: *Eiler et al. (2000); Stracke et al. (2003); Kokfelt et al. (2006); Thirlwall et al. (2004, 2006);* tables 3 & 6. For some samples, $\delta^{18}O_{olivine}$ was calculated from $\delta^{18}O_{glass}$ assuming an olivine-melt fractionation factor of +0.4‰ (e.g. *Eiler, 2001*). Vertical dotted line marks the Pb isotope composition of average eastern Iceland basaltic crust (calculated by averaging analyses of Tertiary lavas from *Kitagawa et al., 2008)*. (d) $^{206}Pb/^{204}Pb$ vs. $^{208}Pb/^{204}Pb$ diagram to illustrate the oblique linear arrays defined by double-spike data on lavas from the Western Volcanic Zone and the Eastern Volcanic Zone that intersect at the 'Enriched Reykjanes Peninsula' component of *Thirlwall et al. (2004)*.

TABLE CAPTIONS

Table 1 Replicate trace element ICP-MS analyses of standard reference materials (BRP-1, JA-1) and an Iceland flank zone lava.

Table 2 Major and trace element data for Icelandic flank zone lavas.

Table 3 New double-spike Pb isotope data for Icelandic flank zone lavas, including Öræfajökull lavas (from *Prestvik et al., 2001*), plus Northern Volcanic Zone tholeiitic and picritic lavas and Eastern Volcanic Zone basalts and rhyolites (from *Kurz et al., 1985; Breddam et al., 2000; Skovgaard et al., 2001*).

Table 4 Sr-Nd-He-O isotope data for Icelandic flank zone lavas.

Table 5 Hf isotope data for Icelandic flank zone and rift zone lavas, including Öræfajökull lavas (from *Prestvik et al., 2001*) and Western Volcanic Zone lavas (from *Peate et al., 2009).*

Table 6 Additional O isotope data on sub-glacial glasses from the Northern Volcanic Zone and other localities (from *Breddam et al., 2000*).

***Table 1**: Replicate analyses of international rock standards and an Iceland sample to assess the precision and accuracy of the ICP-MS trace element data.*

	BRP-1 this study	**± 2 s.d.** n=5	**BRP-1** GeoReM preferred values	**JA-1** this study	**± 2 s.d.** n=4	**JA-1** GeoReM preferred values	**408774** this study	**± 2 s.d.** n=3	**H123** Kokfelt et al. (2006)
Sc	29	2	29	28	1	28	29	3	-
V	396	6	391	103	3	108	304	2	320
Cr	11.6	0.2	12	6.4	0.7	6	383	51	275
Ni	26.2	0.4	23	7.2	0.1	2	124	18	108
Cu	161	2	160	41.0	0.4	41	105	4	-
Zn	144	3	142	86.9	1.3	91	76.6	1.1	79
Ga	25	1	25	16.8	0.3	17	16.2	0.1	-
Rb	35.1	1.1	35.4	10.6	0.2	10.7	10.6	1.2	9.7
Sr	503	12	492	256	2	264	275	1	275
Y	44.1	1.4	42.0	29.0	0.3	29.0	19.5	2.1	16.3
Zr	316	7	310	80.4	0.9	84	102	2	85
Nb	31.2	0.7	29.1	1.45	0.02	1.40	20.1	0.2	18.1
Cs	0.37	0.01	0.37	0.61	0.05	0.64	0.13	0.02	0.12
Ba	552	8	555	302	9	303	142	2	143
La	41.6	0.5	42.6	4.92	0.22	5.00	14.3	0.6	14.3
Ce	92.4	1.3	93.3	13.1	0.3	13.5	31.3	1.0	33.6
Pr	11.8	0.2	12.3	2.10	0.05	2.08	4.08	0.15	4.30
Nd	51.9	0.9	51.9	10.9	0.2	10.9	17.7	0.5	18.2
Sm	11.0	0.2	11.2	3.36	0.08	3.40	3.93	0.18	4.15
Eu	3.33	0.05	3.42	1.11	0.02	1.12	1.30	0.03	1.36
Gd	10.3	0.2	10.4	4.08	0.08	4.20	3.96	0.16	3.98
Tb	1.51	0.01	1.52	0.73	0.01	0.73	0.62	0.02	0.61
Dy	8.53	0.16	8.50	4.80	0.10	4.80	3.72	0.11	3.72
Ho	1.59	0.03	1.62	1.02	0.02	1.05	0.74	0.03	0.74
Er	4.27	0.09	4.20	3.00	0.03	3.00	2.08	0.07	2.03
Yb	3.49	0.09	3.48	2.94	0.06	3.00	1.88	0.06	1.82
Lu	0.50	0.01	0.50	0.45	0.01	0.45	0.28	0.01	0.26
Hf	7.84	0.16	8.00	2.44	0.01	2.50	2.56	0.04	2.51
Ta	1.86	0.05	1.96	0.09	0.00	0.11	1.18	0.01	1.25
Pb	5.66	0.10	5.50	5.85	0.10	5.80	1.09	0.01	1.67
Th	3.76	0.31	3.97	0.68	0.01	0.76	1.19	0.36	1.31
U	0.80	0.01	0.82	0.35	0.04	0.35	0.42	0.01	0.45

Preferred values for BRP-1 and JA-1 are from the GeoReM database (http://georem.mpch-mainz.gwdg.de/).
408774 (*this study*) & H123 (*Kokfelt et al., 2006*) are samples of the same lava flow (Grabrokarhraun) from Snaefellnes.

***Table 2**: Major element (wt%) and trace element (ppm) compositions of Icelandic flank-zone lavas.*

sample	**408738**	**408739**	**408740**	**408744**	**408754**	**408755**	**408757**	**408764**	**408765**
location	Snæfell	Snæfell	Snæfell	Snæfell	Snæfell	Snæfell	Snæfell	SNS	SNS
lat (°N)	64.805	64.807	64.796	64.799	64.817	64.853	64.850	64.893	64.819
long (°W)	15.599	15.590	15.599	15.610	15.697	15.579	15.537	22.332	23.387
SiO_2	47.92	47.81	47.76	47.36	48.08	47.47	47.29	46.65	45.79
TiO_2	1.69	1.93	1.79	1.71	2.02	1.92	2.16	2.06	3.30
Al_2O_3	14.55	15.12	14.95	14.44	15.43	14.47	15.03	14.38	14.39
Fe_2O_3	1.67	2.87	1.56	1.87	1.97	1.95	2.08	2.07	2.43
FeO	8.10	7.92	8.49	8.19	8.92	9.02	9.16	8.17	10.00
MnO	0.17	0.18	0.17	0.16	0.18	0.18	0.18	0.18	0.21
MgO	11.30	8.91	10.49	11.39	8.60	9.70	9.53	10.84	7.86
CaO	10.78	10.96	10.82	10.75	10.76	11.35	10.49	11.58	10.91
Na_2O	2.14	2.34	2.23	2.12	2.41	2.27	2.45	2.25	2.57
K_2O	0.68	0.69	0.66	0.64	0.73	0.64	0.64	0.50	0.94
P_2O_5	0.26	0.28	0.26	0.24	0.29	0.29	0.29	0.42	0.49
total	99.25	98.99	99.19	98.87	99.38	99.25	99.28	99.10	98.99
Sc	32	35	32	34	31	34	32	41	39
V	250	280	266	260	272	276	285	311	437
Cr	730	449	520	645	314	504	529	502	342
Ni	193	124	153	210	122	167	174	302	128
Cu	78	83	85	86	85	80	86	91	66
Zn	74	83	75	71	87	87	81	92	106
Ga	16	19	16	16	18	19	18	16	19
Rb	14.9	13.9	14.3	14.3	15.2	15.3	12.3	9.4	17.1
Sr	360	373	356	351	380	384	380	332	481
Y	18.5	23.1	19.4	18.7	25.1	24.5	21.5	25.7	29.5
Zr	123	137	124	119	152	147	126	115	193
Nb	19.8	22.0	19.4	18.5	24.3	23.3	19.0	23.9	49.1
Cs	0.17	0.16	0.17	0.17	0.17	0.16	0.14	0.10	0.13
Ba	167	186	169	164	196	195	166	166	392
La	16.3	18.0	15.9	15.1	19.5	18.9	15.0	17.4	31.9
Ce	34.9	39.3	34.0	31.2	42.7	41.4	33.2	38.5	68.6
Pr	4.48	5.01	4.46	4.25	5.39	5.30	4.48	5.20	8.53
Nd	19.2	21.7	19.2	17.9	23.4	23.0	20.1	23.1	36.2
Sm	4.32	5.03	4.32	4.17	5.37	5.32	4.64	5.24	7.33
Eu	1.44	1.69	1.47	1.36	1.78	1.76	1.64	1.79	2.51
Gd	4.22	5.03	4.31	4.24	5.31	5.22	4.73	5.35	6.83
Tb	0.64	0.78	0.65	0.62	0.82	0.78	0.73	0.83	0.99
Dy	3.65	4.46	3.75	3.50	4.68	4.73	4.14	4.81	5.63
Ho	0.69	0.85	0.71	0.67	0.89	0.89	0.79	0.95	1.07
Er	1.83	2.27	1.92	1.83	2.41	2.38	2.10	2.60	2.91
Yb	1.56	1.94	1.65	1.50	2.05	2.08	1.79	2.32	2.51
Lu	0.22	0.27	0.24	0.23	0.29	0.30	0.26	0.34	0.37
Hf	2.96	3.41	3.01	2.90	3.71	3.63	3.10	2.94	4.36
Ta	1.11	1.25	1.12	1.05	1.38	1.36	1.08	1.37	2.73
Pb	1.51	1.46	1.78	1.37	1.62	1.53	1.38	1.05	1.61
Th	1.51	1.68	1.48	1.43	1.83	1.79	1.25	1.33	2.22
U	0.46	0.51	0.45	0.45	0.54	0.51	0.36	0.41	0.62

***Table 2 (continued)**: Major and trace element compositions of Icelandic flank zone lavas.*

sample	**408766**	**408767**	**408770**	**408771**	**408774**	**408775**	**408783**	**408784**	**408785**
location	SNS	SNS	SNS	SNS	SNS	Hvamm	Heimay	Heimay	Heimay
lat (°N)	64.845	64.850	64.948	64.976	64.772	63.574	63.404	63.404	63.442
long (°W)	23.740	23.833	22.985	22.675	21.531	19.870	20.275	20.277	20.283
SiO_2	47.27	46.45	46.27	47.25	47.54	46.64	46.42	46.42	46.84
TiO_2	2.03	2.03	1.55	1.88	1.58	2.44	1.64	1.75	1.97
Al_2O_3	13.89	13.55	12.16	13.46	14.76	11.40	14.32	14.62	15.46
Fe_2O_3	2.34	2.28	3.62	2.62	2.42	2.60	2.17	1.29	3.84
FeO	7.84	7.61	6.72	7.61	8.08	9.52	8.97	9.91	7.29
MnO	0.19	0.17	0.18	0.18	0.18	0.19	0.18	0.19	0.18
MgO	11.00	12.12	15.27	12.08	9.89	12.20	11.57	11.06	9.77
CaO	11.57	11.48	10.70	11.38	11.75	11.39	11.45	10.80	10.85
Na_2O	2.12	1.94	1.75	2.02	2.04	2.01	2.18	2.49	2.79
K_2O	0.79	0.91	0.60	0.69	0.51	0.46	0.31	0.41	0.50
P_2O_5	0.45	0.36	0.24	0.30	0.19	0.32	0.16	0.20	0.26
total	99.49	98.89	99.06	99.47	98.95	99.17	99.37	99.13	99.75
Sc	33	39	34	35	29	45	36	30	32
V	289	305	261	282	304	315	291	268	275
Cr	622	961	824	579	383	691	563	545	530
Ni	196	217	282	180	124	266	187	249	182
Cu	88	88	77	80	105	81	79	53	53
Zn	79	67	67	74	77	104	75	77	78
Ga	15	15	13	15	16	16	17	18	19
Rb	16.7	20.6	13.5	15.8	10.6	7.9	5.2	8.2	9.6
Sr	445	474	309	363	275	273	227	262	314
Y	22.4	18.5	17.6	20.8	19.5	24.7	23.9	24.1	26.4
Zr	144	137	106	130	101	137	96	107	130
Nb	40.5	39.9	26.8	31.5	20.1	18.7	9.7	12.8	15.4
Cs	0.18	0.19	0.15	0.18	0.13	0.06	0.06	0.08	0.06
Ba	319	312	198	225	142	102	69	100	118
La	26.9	25.6	17.7	21.1	14.3	14.1	7.80	9.78	12.0
Ce	57.5	53.4	37.7	45.1	31.3	32.9	18.9	23.0	27.8
Pr	7.06	6.49	4.69	5.57	4.08	4.61	2.77	3.25	3.79
Nd	29.6	26.5	19.6	23.6	17.7	21.5	13.3	15.1	17.4
Sm	5.90	5.21	4.05	4.95	3.93	5.39	3.67	3.96	4.43
Eu	2.02	1.67	1.34	1.61	1.30	1.83	1.32	1.39	1.57
Gd	5.41	4.80	3.92	4.70	3.96	5.48	4.14	4.29	4.84
Tb	0.77	0.66	0.59	0.70	0.62	0.86	0.70	0.72	0.80
Dy	4.32	3.67	3.40	3.99	3.72	4.87	4.31	4.39	4.82
Ho	0.82	0.69	0.65	0.76	0.74	0.91	0.87	0.87	0.95
Er	2.23	1.87	1.79	2.08	2.08	2.38	2.40	2.41	2.61
Yb	1.93	1.64	1.63	1.84	1.88	1.95	2.13	2.14	2.27
Lu	0.29	0.24	0.24	0.27	0.28	0.28	0.31	0.31	0.33
Hf	3.32	3.23	2.57	3.10	2.56	3.47	2.51	2.70	3.21
Ta	2.24	2.21	1.51	1.85	1.18	1.11	0.57	0.75	0.89
Pb	1.32	1.58	1.11	1.30	1.09	0.97	0.81	0.96	1.25
Th	2.06	2.38	1.69	1.94	1.19	1.13	0.56	0.76	1.01
U	0.62	0.72	0.50	0.59	0.42	0.37	0.17	0.24	0.33

SNS = Snæfellnes. Hvamm = Hvammsmuli ankaramite (see *Steinthorsson, 1964*)

Table 3: *Double-spike Pb isotope data on Icelandic lavas*

sample	location	flow	Lat °N	Long °W	206Pb/204Pb	207Pb/204Pb	208Pb/204Pb	source of samples
408738	Snaefell	N of Hamar	64.805	15.599	18.6277	15.5030	38.3295	this study
408739	Snaefell	N of Hamar	64.807	15.590	18.4745	15.4931	38.2230	this study
408740	Snaefell	Hamar	64.796	15.599	18.5928	15.5028	38.2988	this study
408744	Snaefell	Hamar	64.799	15.610	18.5949	15.5053	38.3088	this study
408754	Snaefell	Langihnjukar	64.817	15.697	18.4788	15.4961	38.2336	this study
408755	Snaefell	Grabergshnjukar	64.853	15.579	18.4813	15.5020	38.2458	this study
408757	Snaefell	Nalhushnjukar	64.850	15.537	18.4320	15.5000	38.2349	this study
408742	Snaefell	Snaefell	*64.818*	*15.602*	18.5888	15.4995	38.2937	this study
408748	Snaefell	Snaefell	*64.818*	*15.602*	18.4272	15.4883	38.2047	this study
408749	Snaefell	Snaefell	*64.818*	*15.602*	18.5108	15.4931	38.2359	this study
408751	Snaefell	Snaefell	*64.818*	*15.602*	18.4800	15.4905	38.2377	this study
231	Öræfajökull	Öræfajökull	*63.900*	*16.650*	18.5044	15.5361	38.5180	Prestvik et al. (2001)
177	Öræfajökull	Öræfajökull	*63.900*	*16.650*	18.4827	15.5328	38.4679	Prestvik et al. (2001)
67	Öræfajökull	Öræfajökull	*63.900*	*16.650*	18.4810	15.5311	38.4685	Prestvik et al. (2001)
73	Öræfajökull	Öræfajökull	*63.900*	*16.650*	18.5836	15.5336	38.5313	Prestvik et al. (2001)
134	Öræfajökull	Öræfajökull	*63.900*	*16.650*	18.6501	15.5365	38.5635	Prestvik et al. (2001)
138	Öræfajökull	Öræfajökull	*63.900*	*16.650*	18.5506	15.5419	38.5320	Prestvik et al. (2001)
248	Öræfajökull	Öræfajökull	*63.900*	*16.650*	18.5991	15.5418	38.5917	Prestvik et al. (2001)
267	Öræfajökull	Öræfajökull	*63.900*	*16.650*	18.5576	15.5377	38.5746	Prestvik et al. (2001)
136	Öræfajökull	Öræfajökull	*63.900*	*16.650*	18.6479	15.5318	38.5213	Prestvik et al. (2001)
135	Öræfajökull	Öræfajökull	*63.900*	*16.650*	18.6552	15.5310	38.5242	Prestvik et al. (2001)
93	Öræfajökull	Öræfajökull	*63.900*	*16.650*	18.5824	15.5299	38.5182	Prestvik et al. (2001)
408762	Snaefellsnes	Holmshraun	64.859	21.967	18.8329	15.5105	38.4288	this study
408763	Snaefellsnes	Hagahraun (Hitardalur)	64.854	22.024	18.8166	15.5045	38.3967	this study
408764	Snaefellsnes	W of Gullborgarhraun	64.893	22.332	19.0480	15.5287	38.6541	this study
408765	Snaefellsnes	Budahraun	64.819	23.387	18.9678	15.5229	38.6005	this study
408766	Snaefellsnes	NNE of Snaefellsjökull	64.845	23.740	19.0183	15.5323	38.6557	this study
408767	Snaefellsnes	Hreggnasi	64.850	23.833	19.1510	15.5248	38.7662	this study
408768	Snaefellsnes	E of Neshraun	64.856	23.855	18.9799	15.5145	38.5931	this study
408769	Snaefellsnes	W of Hreggnasi	64.849	23.862	19.0307	15.5148	38.6328	this study
408770	Snaefellsnes	Berserkjahraun	64.948	22.985	19.1335	15.5388	38.7567	this study
408771	Snaefellsnes	Svelgsarhraun	64.976	22.675	19.0153	15.5351	38.6488	this study
408774	Snaefellsnes	Grabrokarhraun	64.772	21.531	18.9174	15.5218	38.5197	this study
456713	Eastern VZ	Hvammsmuli	63.574	19.870	19.2155	15.5566	38.8690	this study
408775	Eastern VZ	Hvammsmuli	63.574	19.870	19.2371	15.5631	38.9015	this study
408783	Eastern VZ	Heimey - Storhöfdi	63.404	20.275	19.0467	15.5419	38.6541	this study
408784	Eastern VZ	Heimey - Storhöfdi	63.404	20.277	18.9190	15.5341	38.5460	this study
408785	Eastern VZ	Heimey - Há	63.442	20.283	19.0209	15.5395	38.5862	this study
408786	Eastern VZ	Heimey	*63.417*	*20.278*	19.0621	15.5418	38.6428	this study
408788	Eastern VZ	Heimey	*63.417*	*20.278*	18.9610	15.5314	38.5652	this study
406789	Eastern VZ	Heimey	*63.417*	*20.278*	19.0355	15.5429	38.6133	this study
408790	Eastern VZ	Heimey	*63.417*	*20.278*	19.0519	15.5375	38.6136	this study
408791	Eastern VZ	Heimey	*63.417*	*20.278*	19.0699	15.5427	38.6543	this study
T-30	Eastern VZ	Torfajokull	*63.850*	*19.000*	19.1727	15.5469	38.7842	Stecher et al. (1999)
SK82 13	Eastern VZ	Thrihyrningur	63.775	19.950	19.1736	15.5380	38.7206	Kurz et al. (1985)
SK82 27	Eastern VZ	Sigalda	64.150	19.125	18.4636	15.4629	38.1404	Kurz et al. (1985)
408702	Northern VZ	Kambsfell	64.825	17.768	18.3654	15.4505	38.0632	Breddam et al. (2000)
408706	Northern VZ	Kistufell	64.791	17.175	18.3679	15.4523	38.0337	Breddam et al. (2000)
408707	Northern VZ	Kistufell	64.791	17.175	18.3722	15.4531	38.0500	Breddam et al. (2000)
408709	Northern VZ	Kistufell	64.790	17.176	18.3837	15.4589	38.0596	Breddam et al. (2000)
408710	Northern VZ	Kistufell	64.790	17.175	18.3800	15.4595	38.0579	Breddam et al. (2000)
408712	Northern VZ	Kistufell	64.802	17.209	18.3672	15.4512	38.0488	Breddam et al. (2000)
408713	Northern VZ	Dyngjufjöll Ytri	65.159	16.922	18.3817	15.4537	38.0517	Breddam et al. (2000)
408714	Northern VZ	Dyngjufjöll Ytri	65.160	16.925	18.3787	15.4513	38.0451	Breddam et al. (2000)
408718	Northern VZ	Gaesafjöll	65.753	16.922	18.5098	15.4844	38.2654	Breddam et al. (2000)
408719	Northern VZ	Gaesafjöll	65.753	16.922	18.5035	15.4838	38.2597	Breddam et al. (2000)
408722	Northern VZ	Gaesafjöll	65.756	16.921	18.4982	15.4785	38.2195	Breddam et al. (2000)
408723	Northern VZ	Gaesafjöll	65.756	16.921	18.5078	15.4837	38.2605	Breddam et al. (2000)
408729	Northern VZ	Blafjall	65.488	16.843	18.2064	15.4477	37.8803	Breddam et al. (2000)
408730	Northern VZ	Blafjall	65.488	16.851	18.2102	15.4505	37.8905	Breddam et al. (2000)
408732	Northern VZ	Blafjall	65.518	16.840	18.4580	15.4719	38.2148	Breddam et al. (2000)
408653	Northern VZ - Theistareykir	Klappahraun	65.822	17.034	18.1169	15.4461	37.7903	Skovgaard et al. (2001)
408643	Northern VZ - Theistareykir	Arnahvammurhraun	65.928	17.105	17.9203	15.4125	37.5405	Skovgaard et al. (2001)
408634	Northern VZ - Theistareykir	Theistareykir	65.931	17.074	17.9640	15.4221	37.6138	Skovgaard et al. (2001)
408635	Northern VZ - Theistareykir	Theistareykir	65.932	17.081	17.9637	15.4122	37.5952	Skovgaard et al. (2001)
TH29	Northern VZ - Theistareykir	Theistareykir	65.936	17.061	17.9439	15.4259	37.6021	Skovgaard et al. (2001)
408640	Northern VZ - Theistareykir	Storaviti	65.964	17.101	18.0355	15.4271	37.6885	Skovgaard et al. (2001)
408647	Northern VZ - Theistareykir	Langaviti	65.967	16.899	18.0537	15.4385	37.7330	Skovgaard et al. (2001)
TH40	Northern VZ - Theistareykir	Borgarhraun	65.817	16.905	18.0422	15.4333	37.7286	Skovgaard et al. (2001)
456750	Northern VZ - Theistareykir	Theistareykir picrite	65.920	17.070	17.9360	15.4202	37.5897	this study
MIL-62	Northern VZ - Central Iceland	Illvidrahnjukahraun	65.007	18.688	18.2377	15.4407	37.9068	Chauvel & Hemond (2000)
SK82 06	Northern VZ - Central Iceland	SW of Blagnipa	64.730	19.180	18.3101	15.4512	37.9826	Kurz et al. (1985)
SK82 05	Western VZ - Central Iceland	SW of Blagnipa	64.730	19.330	18.6771	15.4923	38.2764	Kurz et al. (1985)
456702	Western VZ	Hallmundarhraun	64.758	20.783	18.6270	15.4826	38.2210	this study
SK82 28	Western VZ	Kalfstindar	64.237	20.737	18.6851	15.4902	38.2773	Kurz et al. (1985)

latitudes and longitudes in italics indicate aproximate locations

***Table 4**: Sr-Nd-He-O isotopic compositions of Icelandic flank-zone lavas.*

sample	**408738**	**408739**	**408740**	**408744**	**408754**	**408755**
location	Snæfell	Snæfell	Snæfell	Snæfell	Snæfell	Snæfell
$^{87}Sr/^{86}Sr$	0.703554	0.703590	0.703468	0.703604	0.703546	0.703524
$^{143}Nd/^{144}Nd$	0.512988	0.512974	0.512989	0.512993	0.512987	0.512997
εNd	6.8	6.6	6.8	6.9	6.8	7.0
$[^4He] \times 10^{-9}$ ccSTP/g	7.99	4.11	1.19	7.80	2.93	7.13
$^3He/^4He$ R/R_A	6.93	7.12	7.14	7.20	7.02	6.95
± 1 σ	0.10	0.12	0.27	0.10	0.15	0.09
$\delta^{18}O$ olivine	4.61	4.32	4.24	4.07	4.48	4.53
$\delta^{18}O$ plagioclase	-	5.24	-	-	-	5.19
$\delta^{18}O$ clinopyroxene	-	-	-	-	-	4.85
sample	**408757**	**408764**	**408765**	**408766**	**408767**	**408770**
location	Snæfell	SNS	SNS	SNS	SNS	SNS
$^{87}Sr/^{86}Sr$	0.703538	0.703709	0.703457	0.703399	0.703496	0.703400
$^{143}Nd/^{144}Nd$	0.512973	0.512926	0.512957	0.512958	0.512960	0.512934
εNd	6.5	5.6	6.2	6.2	6.3	5.8
$[^4He] \times 10^{-9}$ ccSTP/g	16.3	13.3	1.95	-	3.34	8.42
$^3He/^4He$ R/R_A	7.51	8.52	6.25	-	7.93	8.54
± 1 σ	0.08	0.08	0.16	-	0.11	0.07
$\delta^{18}O$ olivine	4.25	5.08	4.66	-	4.94	5.00
$\delta^{18}O$ clinopyroxene	-	5.37	5.01	-	-	-
sample	**408771**	**408774**	**408775**	**408783**	**408784**	**408785**
location	SNS	SNS	Hvamms.	Heimay	Heimay	Heimay
$^{87}Sr/^{86}Sr$	0.703532	0.703361	0.703335	0.703196	0.703138	0.703169
$^{143}Nd/^{144}Nd$	0.512966	0.512918	0.512987	0.513015	0.513019	0.513030
εNd	6.5	5.5	6.8	7.4	7.4	7.6
$[^4He] \times 10^{-9}$ ccSTP/g	13.8	-	0.10	11.2	4.26	2.08
$^3He/^4He$ R/R_A	8.64	-	17.13	14.51	13.11	13.70
± 1 σ	0.06	-	0.59	0.09	0.15	0.34
$\delta^{18}O$ olivine	4.93	-	4.74	-	5.01	-
$\delta^{18}O$ clinopyroxene	-	-	5.27	-	-	-

***Table 5**: Hf isotopic compositions of Icelandic flank zone and rift zone lavas.*

sample	location	$^{176}Hf/^{177}Hf$	εHf
OR-231 †	Öræfajökull	0.283112	12.0
OR-134 †	Öræfajökull	0.283103	11.7
OR-136 †	Öræfajökull	0.283098	11.5
408738	Snæfell	0.283154	13.5
408739	Snæfell	0.283151	13.4
408740	Snæfell	0.283162	13.8
408744	Snæfell	0.283152	13.4
408754	Snæfell	0.283160	13.7
408755	Snæfell	0.283155	13.5
408757	Snæfell	0.283160	13.7
408764	Snæfellnes	0.283122	12.4
408765	Snæfellnes	0.283122	12.4
408766	Snæfellnes	0.283114	12.1
408767	Snæfellnes	0.283110	12.0
408770	Snæfellnes	0.283113	12.1
408771	Snæfellnes	0.283110	12.0
408774	Snæfellnes	0.283118	12.2
408775	Hvammsmuli	0.283093	11.4
408783	Heimay	0.283103	11.7
408784	Heimay	0.283152	13.4
408785	Heimay	0.283141	13.1
456702	WVZ Hallmundarhraun	0.283197	15.0
456723 ‡	WVZ Reykjanes	0.283202	15.2
456743 ‡	WVZ Reykjanes	0.283155	13.5
456749 ‡	WVZ Reykjanes	0.283151	13.4
456703 ‡	Reykjanes Ridge	0.283267	17.5
456704 ‡	Reykjanes Ridge	0.283251	16.9

† - samples from *Prestvik et al. (2001)*.
‡ - samples from *Peate et al. (2009)*.

***Table 6**: Additional O isotope data on sub-glacial glasses from the Northern Volcanic Zone and other localities.*

sample	location	$\delta^{18}O_{glass}$
408702	Kambsfell	5.17 ‰
408706	Kistufell	4.74 ‰
408707	Kistufell	4.38 ‰
408709	Kistufell	4.60 ‰
408710	Kistufell	4.46 ‰
408712	Kistufell	4.43 ‰
408713	Dyngjufjöll Ytri	3.89 ‰
408714	Dyngjufjöll Ytri	3.91 ‰
408718	Gæsafjöll	3.55 ‰
408719	Gæsafjöll	3.51 ‰
408722	Gæsafjöll	3.46 ‰
408723	Gæsafjöll	3.23 ‰
408729	Bláfjall	5.24 ‰
408730	Bláfjall	5.03 ‰
408732	Bláfjall	3.19 ‰
SK82 05	SW Blágnipa	4.85 ‰
SK82 06	SW Blágnipa	4.91 ‰
SK82 13	Thrihyrningur	5.08 ‰
SK82 27	Sigalda	3.92 ‰
SK82 28	Kalfstindar	4.87 ‰
SK82 29c	Stapafell	5.01 ‰

Sample locations and other information can be found in *Kurz et al. (1985)* and *Breddam et al. (2000)*. Analytical details and standard data can be found in *Breddam (2000)* as these samples were analysed at the same time as the samples of that study.

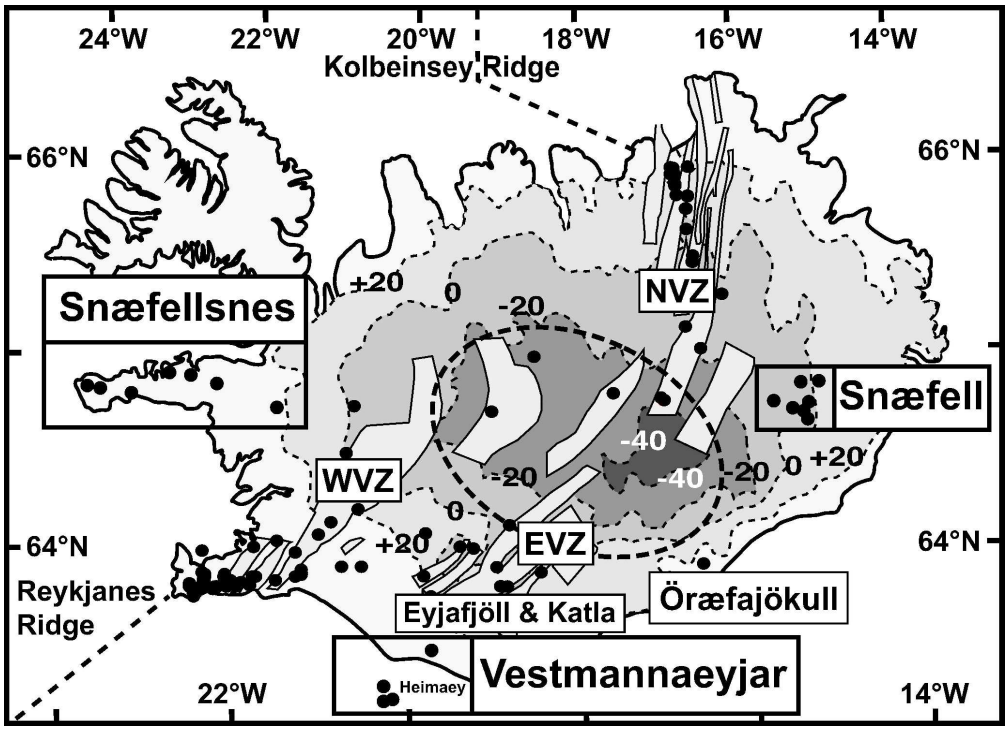

175x126mm (600 x 600 DPI)

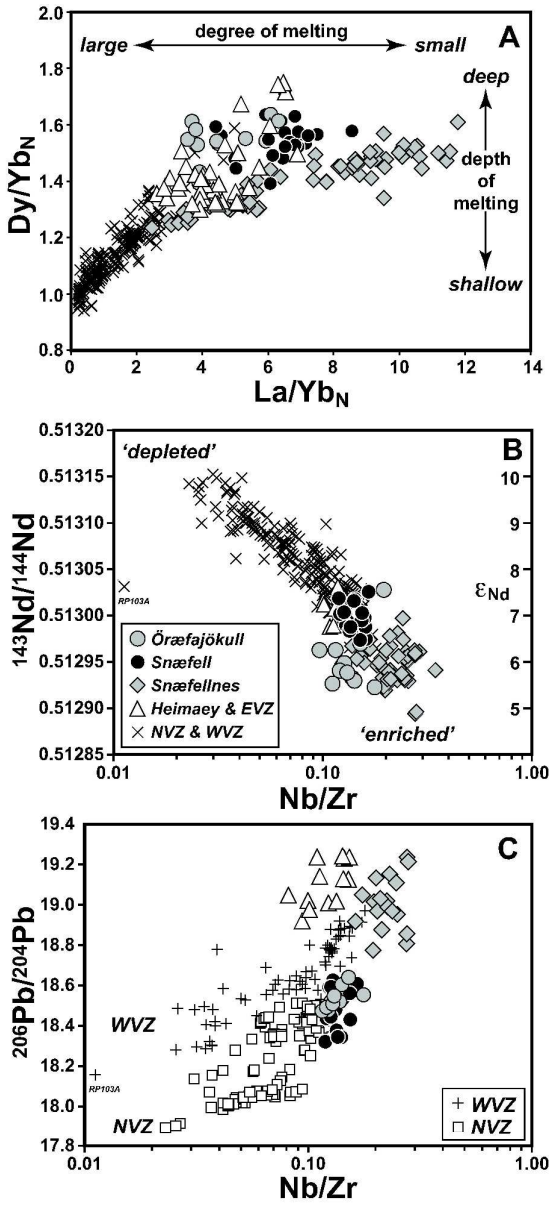

115x253mm (600 x 600 DPI)

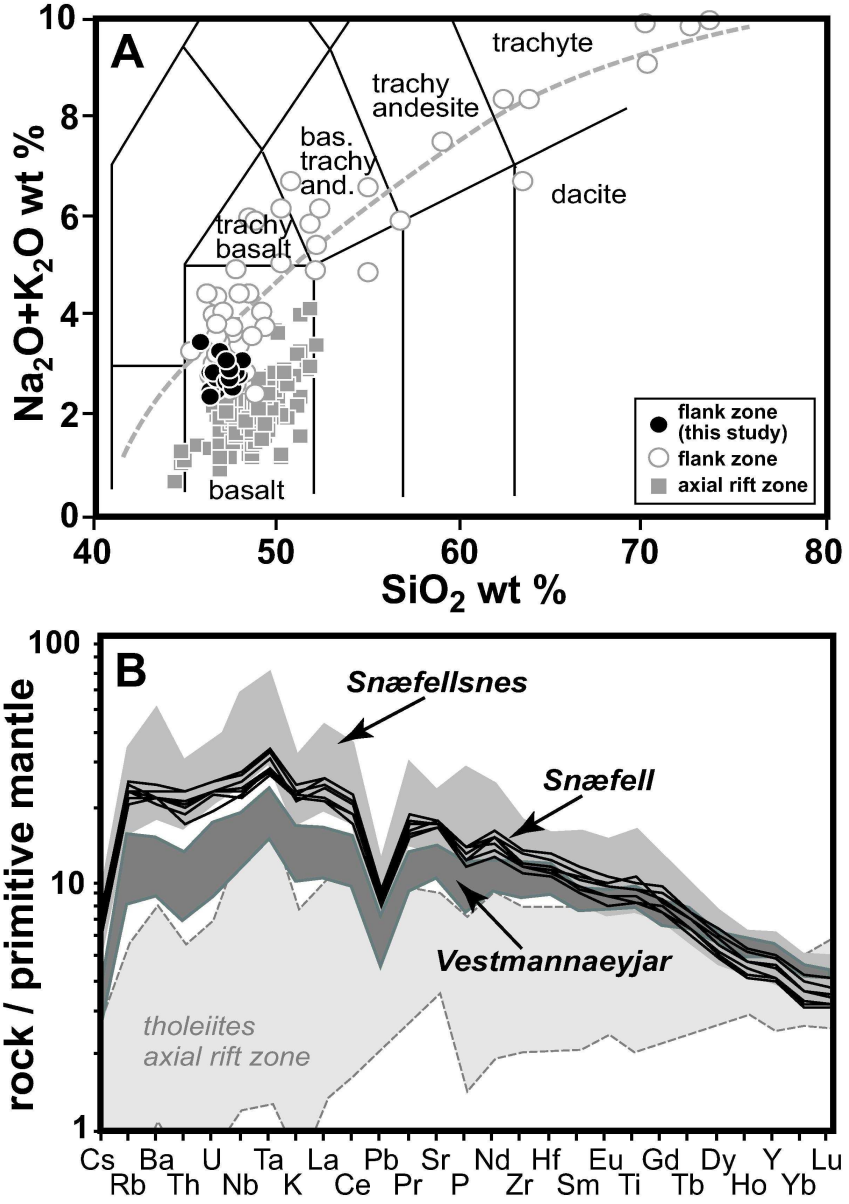

102x145mm (600 x 600 DPI)

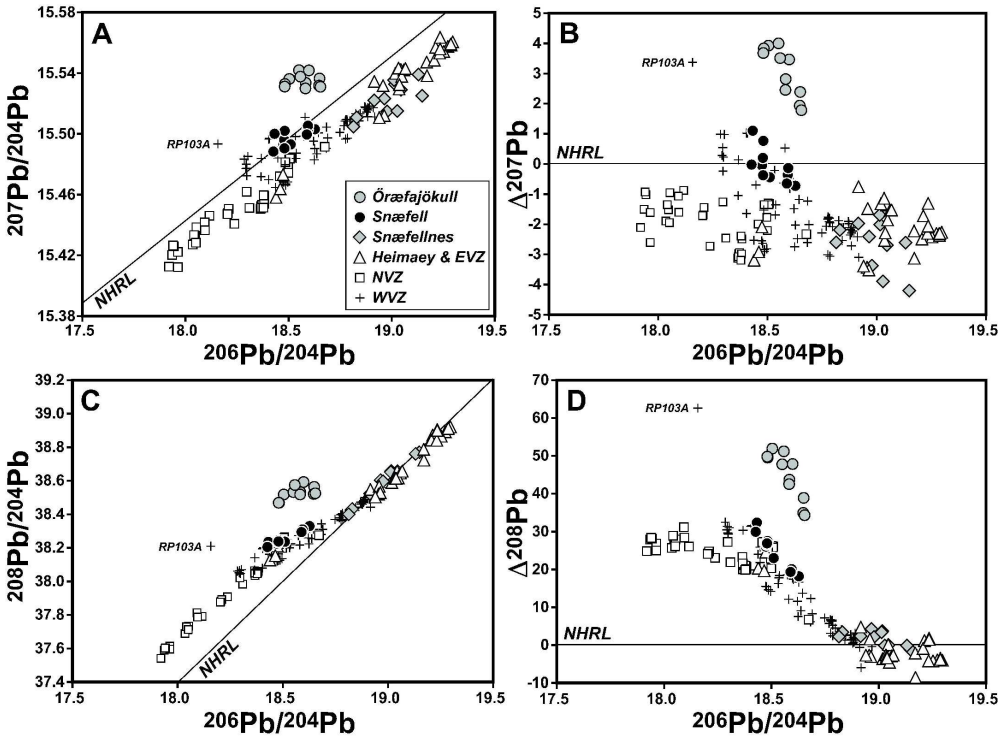

183x134mm (600 x 600 DPI)

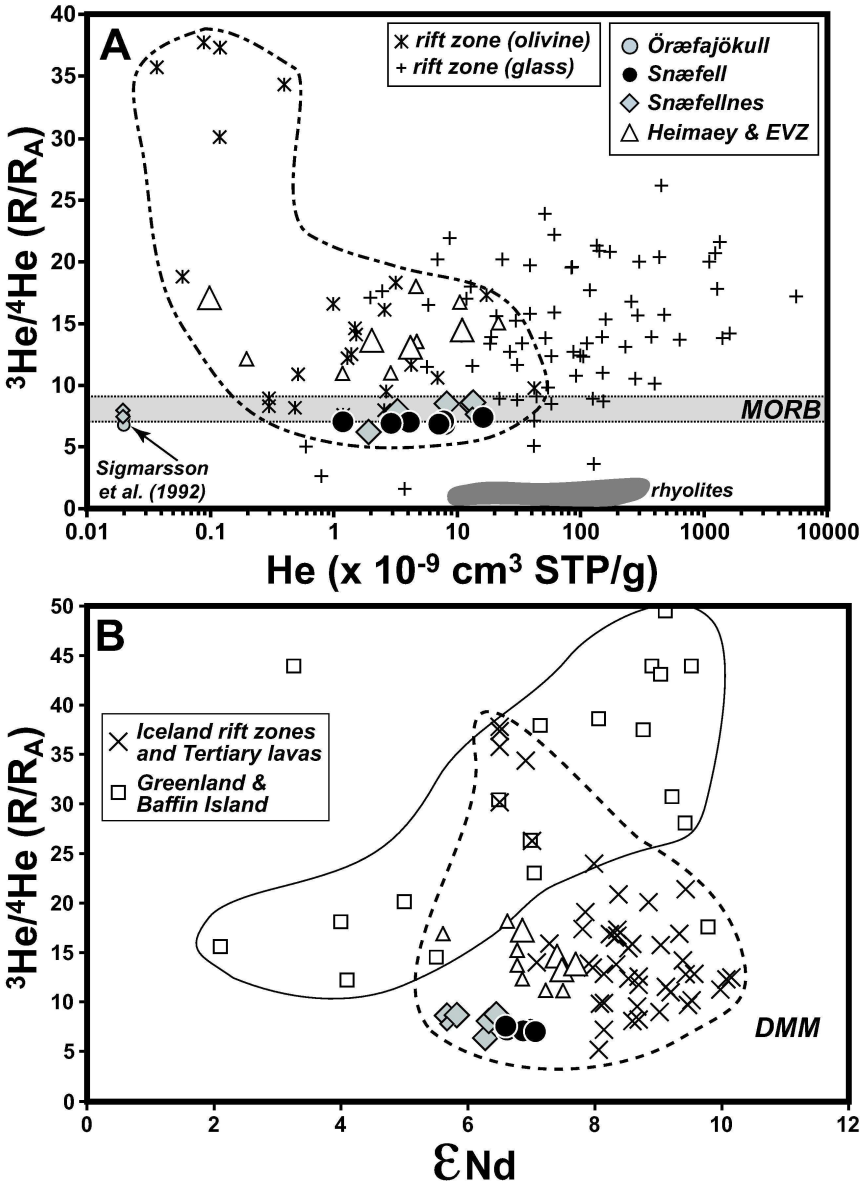

111x154mm (600 x 600 DPI)

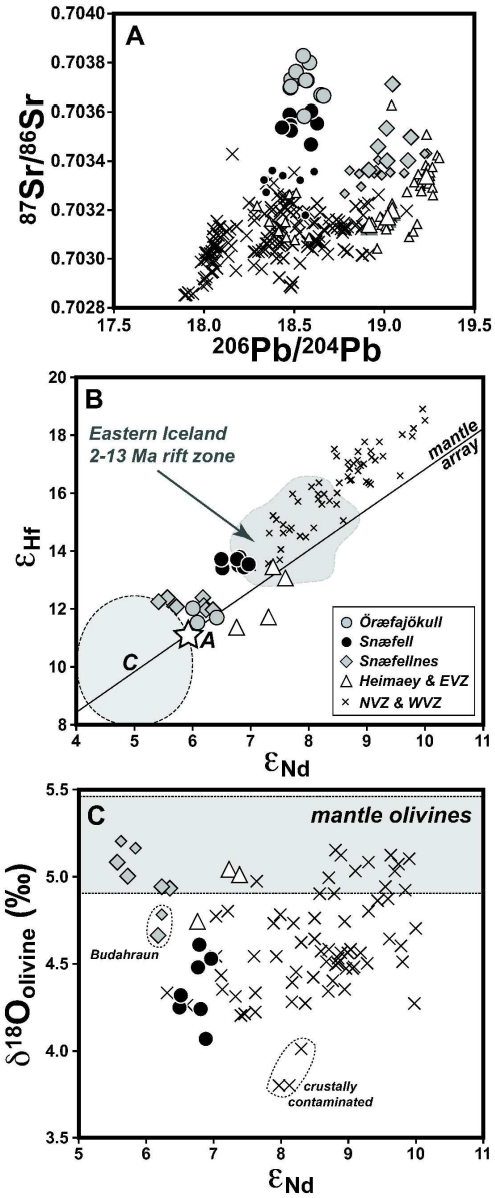

94x226mm (600 x 600 DPI)

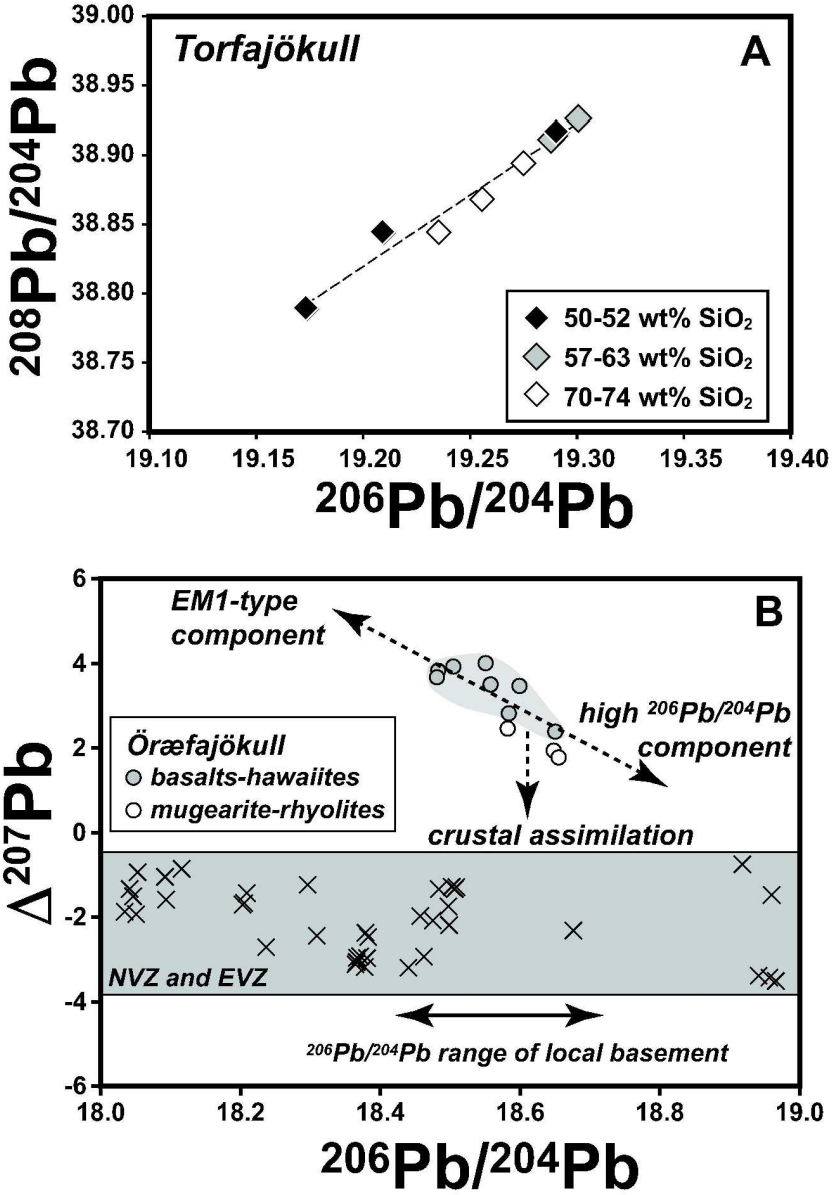

114x160mm (600 x 600 DPI)

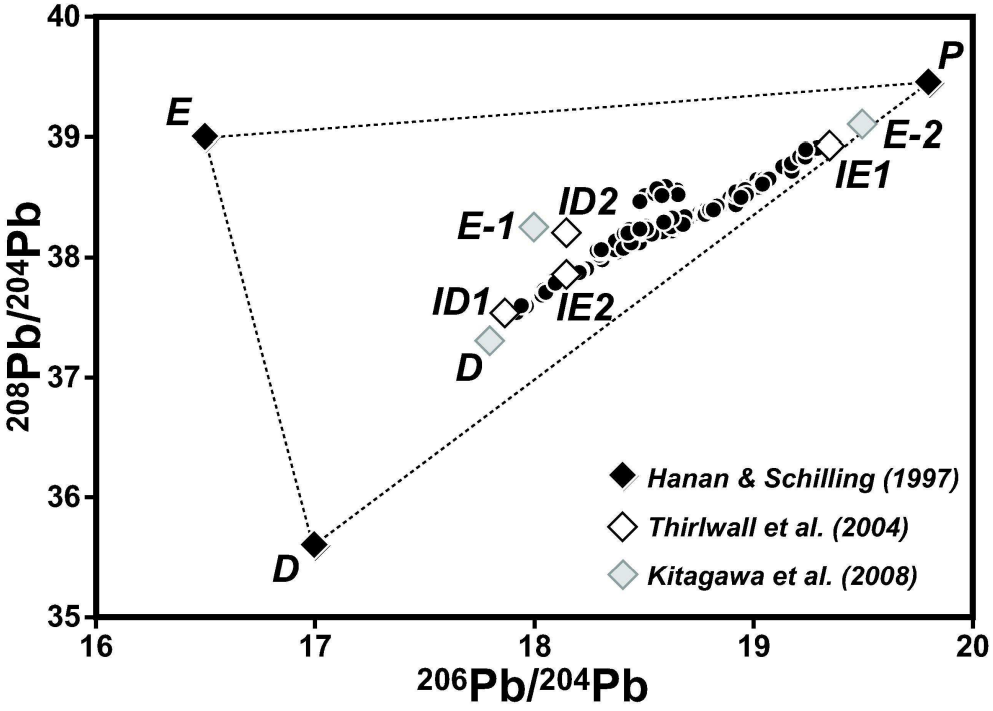

110x78mm (600 x 600 DPI)

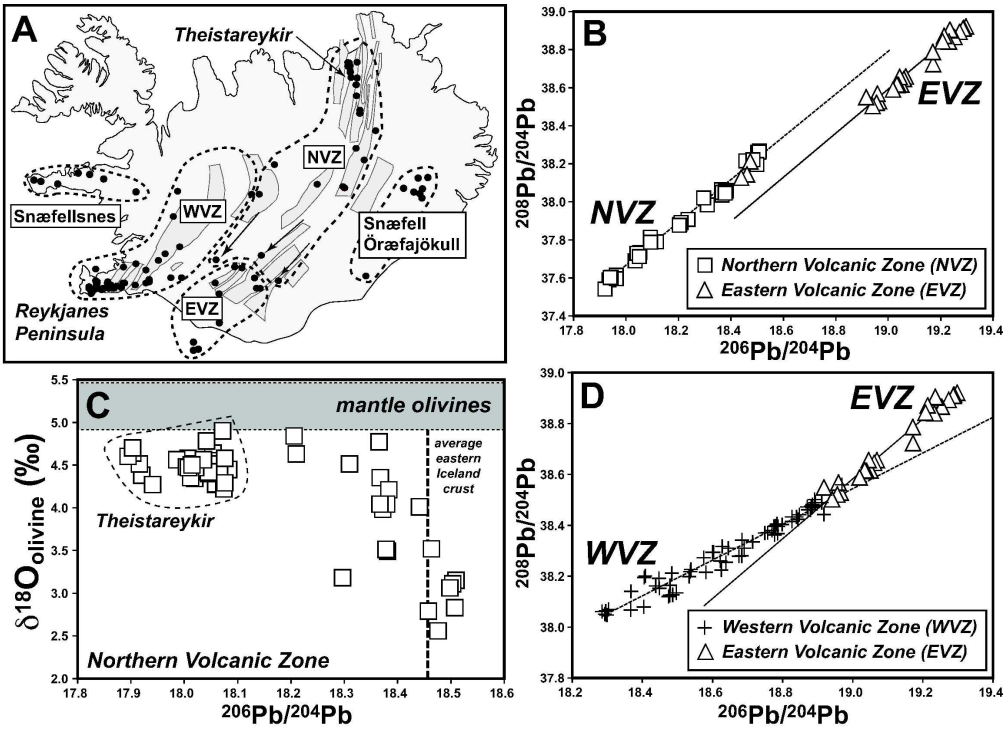

195x141mm (600 x 600 DPI)